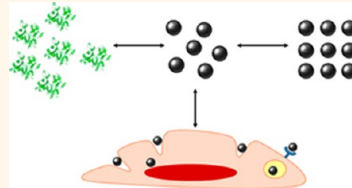


# The State of Nanoparticle-Based Nanoscience and Biotechnology: Progress, Promises, and Challenges

Beatriz Pelaz,<sup>†,‡</sup> Sarah Jaber,<sup>§</sup> Dorleta Jimenez de Aberasturi,<sup>†,§</sup> Verena Wulf,<sup>†</sup> Takuzo Aida,<sup>¶</sup> Jesús M. de la Fuente,<sup>‡</sup> Jochen Feldmann,<sup>#</sup> Hermann E. Gaub,<sup>#</sup> Lee Josephson,<sup>▽</sup> Cherie R. Kagan,<sup>○,♦</sup> Nicholas A. Kotov,<sup>▲</sup> Luis M. Liz-Marzán,<sup>□,★</sup> Hedi MattoSSI,<sup>■</sup> Paul Mulvaney,<sup>§</sup> Christopher B. Murray,<sup>★</sup> Andrey L. Rogach,<sup>⊕</sup> Paul S. Weiss,<sup>∞</sup> Itamar Willner,<sup>||</sup> and Wolfgang J. Parak<sup>†,\*</sup>

<sup>†</sup>Fachbereich Physik and WZMW, Philipps Universität Marburg, 35037 Marburg, Germany, <sup>‡</sup>Instituto de Nanociencia de Aragón, University of Zaragoza, C/Mariano Esquillor s/n, 50018, Zaragoza, Spain, <sup>§</sup>Bio 21 Institute & School of Chemistry, University of Melbourne, Parkville 3010, Australia, <sup>○</sup>Department of Inorganic Chemistry, UPV/EHU, 48940 Bilbao, Spain, <sup>▽</sup>Department of Chemistry and Biotechnology, School of Engineering, The University of Tokyo, 7-3-1 Hongo, Bunkyo-ku, Tokyo 113-8656, Japan, <sup>#</sup>Physik-Department and Center for NanoScience, Ludwig-Maximilians-Universität München, 80799 Munich, Germany, <sup>■</sup>Martinos Center for Biomedical Imaging and the Department of Radiology, Massachusetts General Hospital, 149 13th Street, Charlestown, Massachusetts 02129, United States, <sup>□</sup>Department of Electrical and Systems Engineering, University of Pennsylvania, Philadelphia, Pennsylvania 19104, United States, <sup>♦</sup>Department of Chemistry and Department of Materials Science and Engineering, University of Pennsylvania, Philadelphia, Pennsylvania 19104, United States, <sup>▲</sup>Department of Chemical Engineering, Department of Material Sciences and Engineering, Department of Biomedical Engineering, Biointerface Institute, University of Michigan, Ann Arbor, Michigan 48109, United States, <sup>★</sup>Centre for Cooperative Research in Biomaterials (CIC biomaGUNE), Paseo de Miramón 182, 20009 San Sebastián, Spain, <sup>⊕</sup>Ikerbasque, Basque Foundation for Science, 48011 Bilbao, Spain, <sup>■</sup>Department of Chemistry and Biochemistry, Florida State University, Tallahassee, Florida 32306, United States, <sup>∞</sup>Department of Physics and Materials Science & Centre for Functional Photonics (CFP), City University of Hong Kong, Tat Chee Avenue, Kowloon, Hong Kong S.A.R., <sup>∞</sup>Department of Chemistry and Biochemistry, Department of Materials Science and Engineering, and California NanoSystems Institute, University of California, Los Angeles, Los Angeles, California 90095, United States, and <sup>||</sup>Institute of Chemistry, The Center for Nanoscience and Nanotechnology, The Hebrew University of Jerusalem, Jerusalem 91904, Israel

**ABSTRACT** Colloidal nanoparticles (NPs) have become versatile building blocks in a wide variety of fields. Here, we discuss the state-of-the-art, current hot topics, and future directions based on the following aspects: narrow size-distribution NPs can exhibit protein-like properties; monodispersity of NPs is not always required; assembled NPs can exhibit collective behavior; NPs can be assembled one by one; there is more to be connected with NPs; NPs can be designed to be smart; surface-modified NPs can directly reach the cytosols of living cells.



The still young field of nanoscience has already undergone major advances and breakthroughs. Important discoveries have been made and many questions have been answered. Synthetic protocols for precisely tuning the size, shape, and properties of colloidal nanoparticles (NPs) are now well established. This fine control in the fabrication of NPs has provided researchers with new opportunities for their use as functional building blocks, bringing the properties displayed by NPs on par with those of atoms and molecules. Many NP superstructures with new properties and applications have been developed, mimicking the behavior of efficient natural machines (e.g., enzymes, proteins, biopolymers, or viruses). This idea has had significant impact on several major fields, such as energy and biology. The question that

remains is which direction is nanoscience (based on NPs) heading? In this Nano Focus article, we will highlight the state-of-the-art topics and discuss possible future directions of NP-based nanoscience.

**Nanoparticles Can Exhibit Protein-Like Properties.** Inorganic NPs, with size ranges of 1–100 nm, exhibit size- and composition-dependent properties. For instance, semiconductor NPs and metal clusters exhibit size-dependent absorption and emission features due to size confinement of their electronic states, while larger metal NPs, which contain much larger numbers of electrons, exhibit size- and shape-dependent plasmonic properties. Similarly, NPs made of magnetic materials show size-dependent magnetization. Owing to their discrete electronic states, semiconductor NPs, also referred to as quantum dots (QDs),

\* Address correspondence to [wolfgang.parak@physik.uni-marburg.de](mailto:wolfgang.parak@physik.uni-marburg.de).

Published online September 27, 2012  
10.1021/nn303929a

© 2012 American Chemical Society

have often been termed as “artificial atoms”. When NPs are brought in close proximity to one another their electronic states can couple, which can further alter their individual properties. They can exhibit molecule-like behavior, which leads to the use of the term “artificial molecules” to describe them.<sup>1</sup> Similar considerations can be made for metal NPs, where surface plasmon modes couple and hybridize.<sup>2</sup>

### Narrow size-distribution nanoparticles can exhibit protein-like properties.

Besides the similarity of NPs and their assemblies to atoms and molecules based on electronic states, we can draw further similarities between water-soluble NPs and proteins when considering their interactions with similarly sized macromolecules and their ability to produce complex structural arrangements.<sup>3</sup> Specific proteins can be assigned to an exact chemical formula and thus a precisely defined molecular weight (leaving aside the fact that some of their groups can be chemically modified and statistically protonated/deprotonated). Intramolecular forces between different parts of the protein drive globular proteins into defined structural conformations. Conformations are not rigid, though, as there are temperature-dependent internal modes of fluctuations (protein dynamics). Because of their precise chemical formula and well-defined structural conformation (which can depend on temperature and environment), many proteins can self-assemble and form larger-scale “particles” with long-range order. Depending on the crystallization procedure, the number of proteins per unit cell and the crystal lattice may vary. How do NPs compare to this?<sup>3</sup> First of all, water-soluble NPs and proteins share similar nanoscale dimensions

(see Figure 1a,b) and interfacial chemistry. However, there is also a substantial structural difference between them. Although some small clusters exist that are composed of an exactly defined number of atoms,<sup>4</sup> NPs of one species in general will have some variation in the numbers of atoms in their core, and also some variation in the numbers of attached surfactant molecules on their surfaces.<sup>5</sup> Thus, NPs of one species are usually not identical in their atomic compositions, which distinguishes them from proteins. However, modern synthesis techniques enable preparations of NPs with extremely narrow size distributions.<sup>6</sup> Although this is not absolutely required for successful replication of protein properties, this can certainly help in mimicking their well-defined structure.

Concerning their assembly, the types of forces that determine the interactions of NPs with each other and with their surroundings are the same as those governing proteins. These include van der Waals interactions, dipolar attractions, electrostatic repulsions,<sup>7</sup> and hydrogen bonding. Computer simulations of NP interactions can be built using previous models developed for proteins.<sup>8</sup> The manifestation of the similarity between these interactions and the nanoscale dimensions of NPs can be seen in the self-organization of NPs into superstructures reminiscent of those observed for proteins (see Figure 1c–e).<sup>7,9,10</sup> Without narrow NP size distributions, such superstructures would not form lattices. Also, the issue of the numbers and distributions of capping molecules (surfactants) has a particular relevance in the case of anisotropic NPs, since curvature may vary strongly from one part of the NP to another, and the presence of different crystalline facets may also determine varying adsorption energies. This has been shown to affect the assembly of gold nanorods, toward both forming chains<sup>11</sup> and inducing side-to-side organization.<sup>12</sup>

As an indication of interesting future directions, there are growing numbers of observations of functional

similarities between NPs and proteins,<sup>13–15</sup> although the structural variability of NPs makes their biological function less specific. This disadvantage could be offset by the thermal stability of the NP inorganic cores, which can provide technological advantages in biotechnology and other areas. Understanding where the structural and functional properties are similar and where they are different represents an important fundamental aspect of the concept of NP–protein analogies. Naturally, in our analogy with proteins, solubility of NPs and their colloidal stability is an important issue, which will be discussed below.

We conclude that NP synthesis is already an established field; NPs of extremely high quality in terms of size and shape are readily available for many types of materials, rendering them as flexible building blocks with several advantageous properties that are in many ways analogous to proteins.

**Monodispersity of nanoparticles is not always required.** Having stated above that almost perfectly monodisperse NPs can now be routinely synthesized, one may ask the question: is monodispersity always advantageous? Nature is complex and accommodates both monodisperse as well as polydisperse “molecules”. Naturally synthesized proteins are in general monodisperse (as discussed above), because they are composed of exactly the same number of amino acids, although the structure can vary due to fluctuations and can be controlled by post-translational modification. Molecular identity originates from the way proteins are generated in cells. Specific DNA sequences for corresponding proteins are expressed *via* protein biosynthesis. As each protein of one type is built according to a well-defined genetic code (*i.e.*, the same DNA-based master plan) it has the same sequence of amino acids. Although single-molecule experiments indicate that proteins behave as individual entities (*e.g.*, due to local fluctuations imposed by changes in their nanoenvironments),<sup>16</sup> each protein of one type is designed to fulfill

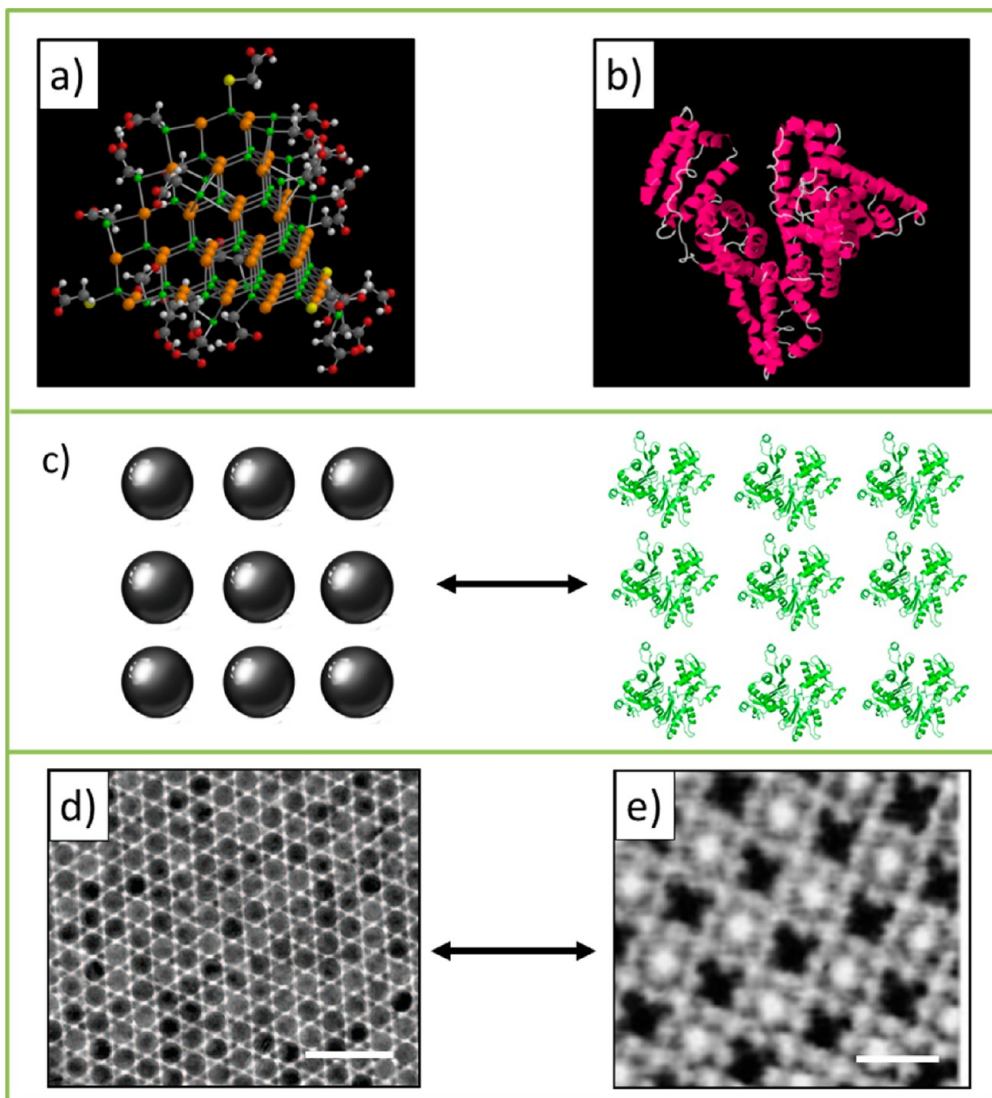


**Figure 1.** (a) Atomic simulation of the core structure of a tetrahedral CdS NP (SPARTAN software). (b) Molecular structure of the protein human serum albumin (Jmol software, RCSB Protein Data Bank, 1AO6). (c) Monodisperse NPs can behave like proteins, for example, in forming 2D lattices. (d) Two-dimensional lattice of 13.4 nm Fe<sub>2</sub>O<sub>3</sub> and 2.5 nm PbSe NPs. The scale bar corresponds to 50 nm. Image reproduced from ref 85. Copyright 2009 American Chemical Society. (e) Two-dimensional lattice of *Bacillus stearothermophilus* NRS 2004/3a/V2 (outer face). The scale bar corresponds to 10 nm. Image reproduced with permission from ref 58. Copyright 1999 Wiley.

the same function, such as enzymatic activity.

Nonetheless, many other types of molecules are polydisperse, such as biopolymers with a distributed number of monomeric motives. Cellulose fibers, for example, provide structural strength, for which the exact length is not critical. Multimeric proteins composed of variable numbers of monomers are thus polydisperse. F-actin and tubulin proteins also do not require a single well-defined length to perform their function as rails for molecular transport. However, the multimeric protein titin is monodisperse, despite its large size.

Titin acts as a ruler for the assembly of the sarcomere with all of the molecular motors in exactly the correct position, and thus, defined length and monodispersity are required. Generally, many molecular assemblies vary their composition according to actual needs. The number of ribosomes translating RNA and the number of stator molecules in the rotary motors of bacteria are just a few examples. Thus, monodispersity of biological molecules is not always required and depends on the respective natural function of the molecule.

Also for NPs, the question of whether monodispersity is required

or not depends on the targeted application, that is, if the required functionality depends on size. This point is nicely illustrated by considering some optical effects of NPs. Titanium dioxide NPs (employed in sunscreen) are used to absorb harmful UV light and to convert it into harmless heat. Although bigger NPs have higher absorption cross sections per NP and thus may provide more effective protection, monodispersity would not necessarily improve protection from UV exposure, as smaller NPs also exhibit sizable absorption. In contrast, the wavelength of emission of QDs strongly depends on size,

and thus, for applications where high color purity is desired (*i.e.*, light-emitting QD-based devices), substantially reduced size dispersity is necessary; reduced size dispersity also prevents detrimental reabsorption. In a variety of applications where light-harvesting properties of semiconductor QDs are important, and, in particular, in those applications related to energy transfer with QDs,<sup>17</sup> size tunability and the precise adjustment of the emission spectrum of the donor toward the absorption spectrum of the acceptor are important.<sup>18–23</sup> Whereas monodispersity is important in the case of devices composed of unannealed NPs such as in the aforementioned QD-based light emitting devices (LEDs),<sup>24</sup> with sintered devices where the NPs are further grown after deposition, such as solution-processed sintered CdTe QD solar cells, increased size polydispersity is less of a concern.<sup>25</sup>

Monodispersity of QDs as fluorescence labels is essential when multiplexed analyses of several targets, such as different mutants or bacteria, are required.<sup>26</sup> For potential medical *in vivo* applications, monodispersity is desirable under certain circumstances. Several organs of the human body act as size-selective filters,<sup>27</sup> exemplified, for instance, by the kidneys and, in particular, by the glomerular basement membranes.<sup>28,29</sup> Small NPs (<5–15 nm) are rapidly and efficiently excreted through the kidneys by renal filtration and are thus eliminated from the body.<sup>30–37</sup> However, large NPs (>200 nm) are easily detected by the immune system, removed from the blood, and delivered to the liver and the spleen, and, to a lesser degree, bone.<sup>38–40</sup> Thus, monodispersity helps to control biodistribution<sup>41</sup> and guide delivery. At the same time, without having well-defined NP sizes, size-dependent cytotoxic effects cannot be properly investigated.<sup>5</sup> In contrast, several commercial NP-based products, such as the aforementioned sunscreen, are not made of

monodisperse NPs, and this limits our ability to access cytotoxic effects of these samples based solely on their physicochemical properties.

Self-organized systems of NPs are examples for which NP “monodispersity” can be desirable but is not strictly necessary. Interestingly, highly polydisperse NPs can give rise to monodisperse *assemblies* as represented by supraparticles (see Figure 2a).<sup>42</sup> These superstructures represent dynamic NP systems in equilibrium (see Figure 2b,c).<sup>43</sup> The balance between the electrostatic repulsion and various weaker attractive interactions results in the formation of equally sized spheres and core–shells from 200–300 individual NPs even though the “building blocks” display wide variations in size.<sup>42</sup> The simplicity of supraparticle assemblies, their multifunctionality, structural versatility, and similarity with viral particles represent interesting directions for future research in nanostructures.

**The simplicity of supraparticle assemblies, their multifunctionality, structural versatility, and similarity with viral particles represent interesting directions for future research in nanostructures.**

We conclude that monodispersity is only required if at least one of the desired functions of the NPs is related to size or to the need for periodic architectures, which ultimately depends on the desired application.

**Assembled nanoparticles can do more than single nanoparticles.** The functional properties of different types of NPs (made from different materials, sizes, and shapes), such as fluorescent, plasmonic,<sup>44</sup> magnetic,<sup>45</sup> biological,<sup>46</sup> and catalytic NPs, have

been reviewed extensively.<sup>47–50</sup> However, besides making use of the individual functionality of the NPs, they can also be self-assembled. As discussed above, supraparticles are one example of such assemblies.<sup>42</sup> Similar to viruses (which they resemble structurally), supraparticles possess a modular structure in which one can combine the functionalities of different building blocks such as semiconductor and plasmonic NPs (see Figure 3a–d).

Colloidal crystals are examples of assemblies of NPs that can exhibit novel and better properties in comparison to individual NPs. The basis of colloidal crystals is that NPs have predominantly isotropic interparticle interactions. Owing to extremely narrow size distributions, self-assembled colloidal crystals can reach three-dimensional (3D) lattices with millimeter-scale dimensions (*i.e.*, macroscopic, see Figure 3e). Another type of self-assembly is based on anisotropic NP interactions, mostly characteristic of water-soluble NPs. They do not have to be monodisperse, yet they self-assemble into a large variety of superstructures based on the preferential patterns of NP attachments to each other. Initially, researchers demonstrated the assembly of NPs in chains and nanowires,<sup>7</sup> and subsequently, a family of NPs self-assembled into sheets,<sup>9</sup> and more complex 3D superstructures exemplified by gels<sup>51</sup> and twisted nanoribbons were reported.<sup>10</sup> Besides the cases of assembly under the influence of external forces, the self-organization of NPs can also be induced by forces from other molecules, as in excluded volume interactions,<sup>52</sup> which can be used for fine-tuning the patterns and dimensions of assembled structures.

One way to control the interparticle spacing in these assemblies is the use of a spacer such as a polymer or microgel. For example, core–shell microgels have well-defined structures that consist of a single NP core with a polymer shell. The effective particle volume thus increases, providing a spacer between

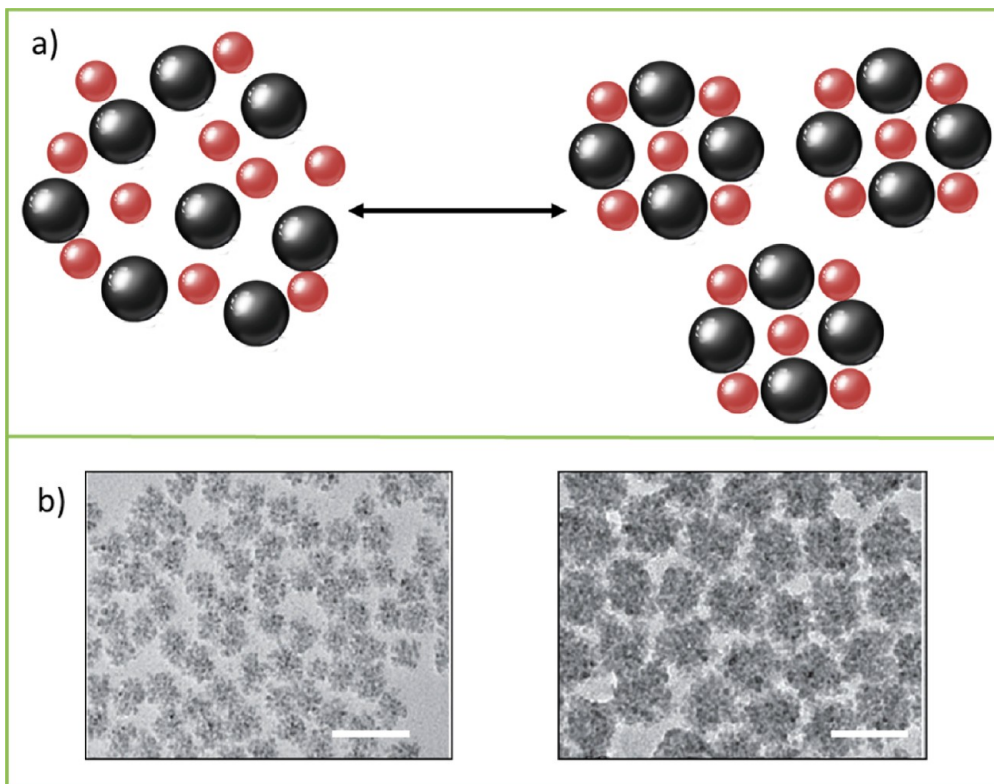


**Figure 2.** (a) Nanoparticles with broad size distributions can assemble into quasi-monodisperse particles. (b) Assembly of core-shell supraparticles from CdSe and Au NPs. The scale bars correspond to 50 nm. Images are reproduced with permission from ref 42. Copyright 2011 Nature.

the NP cores that becomes important for controlling nearest-neighbor distances in the self-assembly.<sup>53,54</sup> Especially useful are responsive microgels where the volume can be tuned through external stimuli such as pH, temperature, or ionic strength. This then provides two ways of controlling particle distances: first by controlling the size of the spacer through synthesis, and second through the use of external stimuli. Discrete NP assemblies analogous to regular molecules can also be made with great precision using DNA connectors.<sup>55,56</sup>

While the previous examples considered direct self-assembly of NPs both with and without specific interparticle linkers, self-assembled templates can also be used, to which the NPs are subsequently bound.<sup>57</sup> A classic set of templates are two-dimensional (2D) crystals of S-layer proteins, which, depending on the experimental conditions, can be formed with different lattice types.<sup>58</sup> Nanoparticles can later be attached to periodic structures and thus

periodically assembled.<sup>59</sup> Another example of 2D protein crystals are chaperonin templates. Engineering the pore size of the barrel-like protein structure enables the assembly of NPs with different sizes.<sup>60</sup> Use of DNA bridging offers even more flexibility for designing one-dimensional (1D), 2D, and 3D templates.<sup>61</sup> Beyond lattices, more sophisticated structures are possible. For example, single-stranded DNA, which exhibits predesigned complementarity, self-assembles into 2D sheets that roll over into single DNA tubes of controllable diameters, similar to the formation of carbon nanotubes (CNTs) from graphitic sheets. By using "sticky" ends protruding from the DNA lattice (*i.e.*, by the modification of the DNA subunits with protruding nucleic acid tethers), NPs can be attached.<sup>62,63</sup> For example, Au NPs could be hybridized with the subunits of the tubes to form "honeycomb" NP/DNA tube nanostructures.<sup>64</sup> These concepts ultimately lead to the development of DNA-origami

templates, which are not necessarily bound to surfaces.<sup>65</sup> These can be used as templates that enable NP assembly in 3D.<sup>66</sup>

While the direct self-assembly of NP lattices (without linkers) offers only a limited degree of freedom concerning the spacing between the individual NPs and the composition of the lattice out of different types of NPs, attachment of NPs to self-assembled templates enables convenient tuning of inter-NP distances. This strategy has been employed for measuring distance-dependent quenching effects.<sup>67</sup> However, because of their intrinsic size, templates cannot provide the same small distances between NPs as are possible in directly self-assembled NP structures. Therefore, depending on the application, one or both approaches can be selected.

Controlled NP assemblies lead to materials with novel properties, due to coupling effects exhibited by NPs in close proximity. In the case of fluorescent, semiconducting, plasmonic,

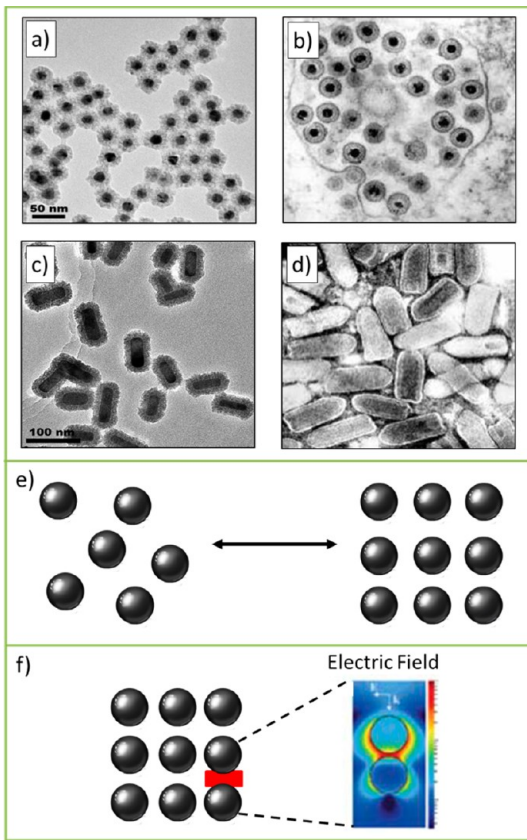


**Figure 3.** Transmission electron microscopy images of (a) self-assembled monodispersed supraparticles of CdS (shell) and Au (core). The scale bar corresponds to 50 nm.<sup>42</sup> (b) Herpes simplex virus magnification ca. 40000 $\times$ , with remarkable structural similarity to the supraparticles as shown in image a. Micrograph from F. A. Murphy, School of Veterinary Medicine, University of California, Davis. (c) Composite NPs made out of a CdSe (shell) and Au nanorods (core). The scale bar corresponds to 100 nm.<sup>42</sup> (d) Rabies virus. Magnification ca. 40000 $\times$ , with similar structure to the composite NPs shown in image c. Micrograph from F. A. Murphy, School of Veterinary Medicine, University of California, Davis. (e) Nanoparticles can be assembled into periodic structures, such as 2D lattices. (f) If plasmonic NPs are brought into proximity, an incident electromagnetic field can be amplified between the NPs, at so-called hot spots (as depicted in red). The distribution of the electric field between the Au NPs is shown. Image adapted with permission from ref 48. Copyright 2011 RSC Publishing.

and magnetic NPs, excited electronic states and magnetic moments couple to one another. By using assembled QDs with different wavelengths, fluorescence resonance energy transfer (FRET) between adjacent QDs can be used to funnel light from high to low energies.<sup>68–70</sup> With the recent introduction of compact ligands that promote strong interparticle coupling and methods to dope QDs,<sup>71–73</sup> NP assemblies integrated into field-effect transistors have shown high-carrier mobilities exceeding 15 cm<sup>2</sup>/(V s) and the benchmarks of conventional thin film amorphous silicon transistors.<sup>74,75</sup> In the case of plasmonic NPs, plasmons of adjacent NPs can couple, leading to enhanced plasmonic

heating<sup>76,77</sup> or hot spots for surface enhanced Raman scattering (SERS) and fluorescence<sup>78,79</sup> enhancement (see Figure 3f).<sup>80,81</sup> Coupling of magnetic moments between adjacent NPs can lead to changes in their collective relaxivity.<sup>82,83</sup> Thus, in all cases, the coupling of NPs changes their properties. Other interesting directions originating from changing the properties of NPs through their arrangement is the concept behind chiral NPs<sup>84</sup> and their assemblies,<sup>85,86</sup> which were observed only recently. Here, 3D assembly of NPs can lead to chirality, a property that is not specifically controlled in the NP building blocks.<sup>66,87–89</sup> In this case, though, there is no coupling between the

assembled NPs: it is the interaction of light with the NP assembly that alters the assemblies' properties to be distinct from those of individual NPs. Understanding the origins of the chiral properties of NPs and their relation to those of typical carbon-based structures<sup>90</sup> for both semiconductor and metallic nanostructures is likely to generate much interest in the future.

Cluster-assembled materials represent a limit of precise assembly and controlled coupling.<sup>91</sup> In this case, precisely stoichiometrically defined clusters (e.g., As<sub>7</sub> or Au<sub>11</sub>) are held together by ionic, covalent, or other well-defined linkers. As the clusters are relatively distant, their coupling is not strong and the calculated and measured bands are relatively flat. Nonetheless, by varying the linkers for a specific cluster, the material properties, such as the band gap, can vary dramatically.<sup>92,93</sup>

We conclude that the integration of individual NPs into larger, submicrometer-, micrometer-, or millimeter-sized objects can provide new functionality, not exhibited by individual NPs. Integrative structures can be assembled massively in parallel structure. In addition to random assembly, both directed assembly and the use of self-assembled molecular structures as templates are possible, thus enabling creation of functional materials from existing NP building blocks.

**The integration of individual NPs into larger, submicrometer-, micrometer-, or millimeter-sized objects can provide new functionality not exhibited by individual NPs.**

**Nanoparticles can be assembled one-by-one.** While for some applications dispersed NPs in solution are required,

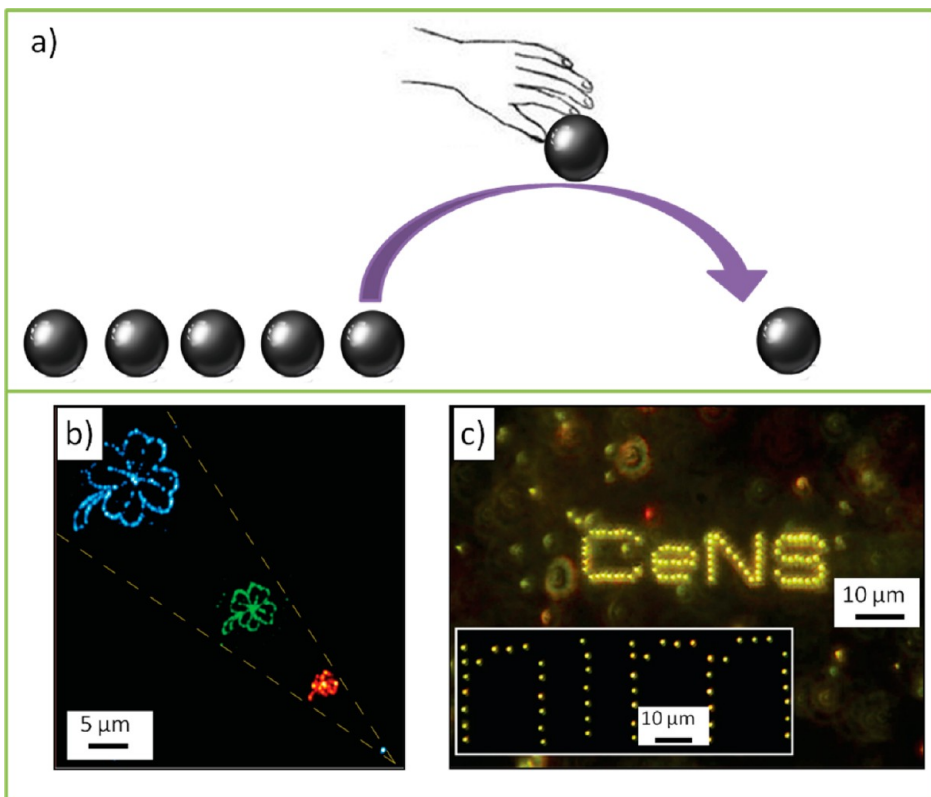


**Figure 4.** (a) Nanoparticles can be assembled one by one on surfaces. (b) Pattern of fluorescent NPs assembled by AFM. Image reproduced from ref 99. Copyright 2008 American Chemical Society. (c) Pattern of plasmonic NPs assembled by laser deposition. Image reproduced from ref 101. Copyright 2010 American Chemical Society.

such as *in vivo* delivery, for other applications, such as molecular electronics, NPs need to be assembled on surfaces (see Figure 4a). Although NPs can serve as individual functional building blocks, as for single QD transistors,<sup>94</sup> for the creation of functional devices, NP components need to be positioned and connected. Parallel assembly was described in the sections above for the creation of ordered, periodic structures, or randomly assembled NPs, but some applications require higher degrees of control over the pattern formation. Ultimately, one-by-one assembly of NPs on surfaces may be desired. There has been much discussion centered on the idea of assembling structures atom-by-atom.<sup>95–98</sup> Even though the assembly of free-standing 3D structures may have intrinsic limitations, there have been several instances where assembly of 2D structures on surfaces has been successfully demonstrated. This work started with advances in scanning probe microscopy. These microscopy techniques

were initially developed to image surface structures; more recently, interactions between the probe tip and the target sample/specimen have also been manipulated. With the probe tip of a scanning tunneling microscope (STM), individual atoms can be moved to a designated location on the surface.

In general, in STM manipulation the greatest problem is not moving the building blocks with the probe tip, but rather releasing them once the desired position has been reached.<sup>95</sup> Forces initially have to be adjusted so that the adhesive force between the probe and the object is larger than that between the object and its underlying substrate. For release at the target location, the situation needs to be reversed in order for the object to adhere more strongly onto the substrate. For transporting atoms with the tip of an STM, the interaction between probe tip and object can be tuned by adjusting the electric potential applied to the STM tip. The same concept is more difficult for

larger objects, such as NPs.<sup>99</sup> However, with the application of hierarchical forces, bigger objects, such as biological molecules or NPs, can be assembled one-by-one into pre-designed patterns using an atomic force microscope (AFM, see Figure 4b). The strategy here uses molecular linkers of different binding strengths that are attached to the building block. Pulling on a chain ultimately breaks the weakest link. Oligonucleotides are convenient linkers, as their binding strengths to DNA depend on the length of the strand and on the orientation of the applied force.<sup>100</sup>

**Bigger objects, such as biological molecules or NPs, can be assembled one-by-one into predesigned patterns.**

Interactions of NPs with light present a conceptually different

approach, in which NPs are trapped in a focused light beam and pushed to a surface. Recent experiments on laser printing have opened new perspectives for patterning surfaces with metal NPs (see Figure 4c).<sup>99,100</sup> Tuning the wavelength of the trapping laser into resonance with the plasmon frequency of gold NPs leads to repulsive scattering forces dominating trapping gradient forces. As a consequence, single gold NPs can be pushed by light in the forward (light propagation) direction.<sup>101</sup> In the vicinity of a charged surface, this leads to light-controlled printing of single NPs with a precision of several tens of nanometers.<sup>101</sup> This serial optical printing technique can be extended to parallel printing by introducing 2D spatially segmented liquid-crystal modulation of the expanded beam and by applying the appropriate spatial modulation patterns.<sup>102</sup> Such novel printing strategies will become a versatile and cost-effective tool for future fabrication of nanoplasmnic device structures.

Arrangements may also be composed of a combination of different NPs with functional biomolecules like proteins or aptamers. The combination of enzymes with catalytic NPs promises novel synergistic effects arising not only from the chosen composition but even more so from the precise spatial arrangement of the components. Designer cellulosomes<sup>103</sup> are envisioned where the bacterial multicomponent enzyme machinery, which degrades lignocellulose with unparalleled efficiency, is mimicked in a synthetic biology approach in the sense of “learning by building”, with potential applications in renewable energy. In contrast to parallel assembly, sequential arrangement of NPs enables full flexibility in arranging them. The main drawback is the slow speed of assembly.

We conclude that complex objects such as NPs can be sequentially assembled one-by-one on surfaces to form 2D patterns. Writing 2D structures with NPs is possible and will find use in basic and applied research.

**There is more to be connected with nanoparticles.** NPs need to be interfaced with the environment. In the field of energy, NPs often have to be embedded into a polymer matrix in order to form a device. In particular, in solar-cell applications,<sup>104</sup> interactions of QDs with the surrounding matrix have important effects that can be used to adjust energy transfer with charge separation in the composite structure,<sup>105,106</sup> to serve as components in conducting windows,<sup>107</sup> and to improve the performance of the resulting devices.<sup>108</sup>

In the popular field of biorelated applications, NPs are preferentially dispersed in biological fluids (such as blood). Colloidal stability and specific interactions with the environment (such as targeting) are typically provided by conjugation of molecular ligands and biological molecules (e.g., enzymes or antibodies) to the surfaces of the NPs. Strategies for providing their colloidal stability can be grouped into two categories: encapsulation and ligand exchange.<sup>109</sup> Encapsulation within block copolymer shells and phospholipid micelles exploits the natural ability of a variety of bifunctional amphiphilic molecules (including block copolymers and phospholipid micelles) that present chemically distinct segments in their structures, one being hydrophobic while the other is hydrophilic.<sup>110–114</sup> To minimize their energy, these molecules line up at the interfaces between hydrophobic and hydrophilic media. This interfacing manifests itself at the nanoscale and is suitable for the assembly of colloidal NPs, such as semiconductor QDs, and magnetic and plasmonic NPs. For instance, when mixed with hydrophobic NPs, the hydrophobic segments preferentially interact with the native ligands (creating strong entropy-driven association), while the strong affinity of the hydrophilic segments to water molecules promotes the dispersion of the NPs in buffer media. Some of the common means to promote compatibility with water are based on inserting charged groups (such as amine or

carboxyl groups) and/or poly(ethylene glycol) (PEG) chains within the hydrophilic segments. In several instances, these polymers are prepared by substituting some of the carboxyl groups with alkyl chains to balance the hydrophobic and hydrophilic blocks within the polymer chains.<sup>111,115</sup> Such balance is critical for the stabilization of the polymer coating on the hydrophobic ligands and for the promotion of water solubility of the resulting NPs.

Ligand exchange, on the other hand, involves the substitution of the native surface cap with hydrophilic bifunctional molecules and oligomers (ligands).<sup>116–123</sup> The molecules present anchoring group(s) at one end that coordinate the NP (Lewis-base interactions, typically thiol, carboxy, and amine groups) and hydrophilic groups at the other end (e.g., carboxylic acids, amino acids, PEGs); the latter promote affinity to buffer media. Some early examples of this strategy included the use of mercaptoundecanoic acid, dihydrolipoic acid, thiol-appended dendrons, and small cysteine ligands.<sup>118,119,124,125</sup> The use of thiol–alkyl–carboxylic acid ligands to promote the transfer of NPs to water is simple to implement. However, the long-term stability of the resulting NPs is strongly dependent on the affinity of the anchoring groups to the NP surfaces.<sup>126</sup> The introduction of modular ligand structures, containing one or more dihydrolipoic acid (DHLA) groups at one end of the PEG chain for strong anchoring onto the QD surface, and a biocompatible group at the other end of the PEG, substantially improves the colloidal stability of these materials. These surface modifications have enabled straightforward access to biological molecules through avidin–biotin binding or 1-ethyl-3-(3-dimethylaminopropyl) carbodiimide (EDC) coupling. While several well-established approaches for providing NPs with excellent colloidal stability in biological liquids are available,<sup>114</sup> routine conjugation to biological molecules remains challenging.



**Figure 5. Photograph of water-based material with shape memory.** Image adapted with permission from ref 127. Copyright 2010 Nature.

These fascinating materials have thus far been scarcely explored in the context of NPs. One example is water-based materials (see Figure 5). For the realization of a sustainable society, one may consider water as a source for plastic materials. In particular, as alternatives to polymers, ultralow-organic-content hydrogels, consisting mostly of water, are attractive if they are sufficiently strong and can be processed into any shape. The first example of such water-based materials, reported in 2010, makes use of clay nanosheets in combination with an organic binder for constructing 3D networks leading to hydrogelation.<sup>127</sup> This design strategy may allow incorporation of a variety of functional nanoscale motifs such as NPs, nanorods, and even enzymes for a wide range of applications.

We conclude that although NPs have been combined with many different materials for forming composite materials within the last two decades, as Feynman said, "There is plenty of room at the bottom," and exploration of novel combinations lies ahead of us.

**Nanoparticles can be designed to be smart.** It can be argued whether some NPs can be defined as "smart". In this section, recent developments in NPs for biological applications will be discussed, followed by arguments regarding what makes the NPs smart. Again, a key requirement for NPs in the context of biological applications is colloidal stability and appropriate interfacing with the biological

environment, which is typically achieved *via* conjugation to functional biological molecules.

One possible criterion for arguing that a NP is smart entails that, in addition to providing a platform for arraying several types of functional molecules, the physical and/or chemical property intrinsic to the NP can be altered or modulated by the environment. A simple case involves the use of fluorescent NPs for the purpose of imaging or tracking. Locations of the NPs can provide a visualization vehicle (*via* fluorescence), which is used in cellular immunostaining,<sup>128</sup> delivery, *in vivo* contrast,<sup>129</sup> and tracking of membrane surface receptors.<sup>130</sup> The NP then becomes "smart" when its emission becomes dependent on its microenvironment. In sensing, several "smart" NP architectures have been introduced. For instance, pH-sensitive

QD-bioconjugates can effectively report on pH changes in solution, within the cytoplasm of fixed cells or intracellular compartments (see Figure 6a,b).<sup>131–134</sup> The local pH can vary significantly between different cellular compartments or different organs. NPs experience a strongly acidic environment inside endosomes/lysosomes of live cells, whereas NPs in extracellular fluids or inside the cytosol essentially experience neutral pH. Thus, the fact that fluorescence depends on the pH can provide information about the location of the NPs. This could provide a convenient tool for investigating the pathways involved in the NP uptake by live cells, as NPs that are directly delivered to

the cytoplasm experience neutral pH, while those endocytosed experience more acidic environments.<sup>114</sup> Likewise, chemically modified QDs can follow intracellular metabolism by turning on the fluorescence of the NPs in response to cell-generated 1,4-dihydro-nicotinamide adenine dinucleotide (NADH). Implementation of such "smart" NPs for intracellular anticancer drug screening was recently demonstrated.<sup>135</sup>

Integrated sensors can also help to monitor the function of NPs. Enzyme-modified NPs can be used for locally processing respective substrate molecules. Protons are a by-product of many enzymatic reactions. Thus, by integrating pH-sensitive fluorescence into enzyme-conjugated NPs, substrate turnover upon enzymatic processing can be monitored by NP fluorescence (see Figure 6c).<sup>134,136</sup> The growth of metal NPs on metallic catalytic seeds by enzymatic transformation has been demonstrated, and the plasmonic absorbance of the resulting NPs was extensively used to sense different analytes, such as glucose, neurotransmitters, or the NADH cofactor.<sup>137,138</sup> The incorporation of Au NPs into cancer cells and the intracellular NADH-mediated growth of core–shell Au/Cu NPs enabled optical probing of intracellular metabolic pathways *via* resonance Rayleigh scattering, using dark-field microscopy.

Metal NP/enzyme hybrids can impact other areas in nanobiotechnology beyond sensing. Metal NP/enzyme hybrids have been used as "smart" inks for dip-pen nanolithography patterning of surfaces.<sup>139</sup> The biocatalytic growth of the NPs on the biomolecular templates generated micrometer-long metallic nanowires. In contrast to electroless synthesis of nanowires, proceeding in a noncontrolled process, the biocatalytic growth of the nanowires includes a self-inhibiting growth mechanism, leading to nanowires controlled by the enzyme-template dimensions. By applying different enzymes, the orthogonal deposition of different compositions of nanowires

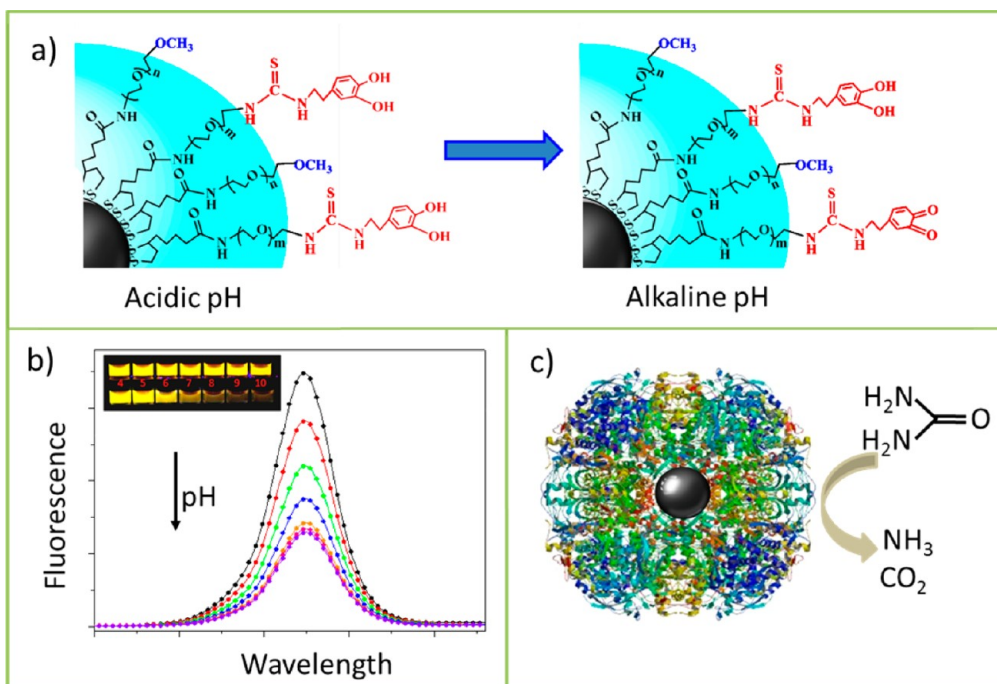


**Figure 6.** (a) Charge-transfer interactions between fluorescent QDs and redox-active dopamine lead to pH-dependent quenching of QD fluorescence by dopamine. (b) This effect can be used as a pH sensor. Image reproduced from ref 134. Copyright 2012 American Chemical Society. (c) Similar pH-sensitive QDs can be used for detecting enzymatic reactions. Smart enzyme-modified QDs are used to detect enzymatic reactions, triggered by sensing the surrounding pH. Image reproduced from ref 136. Copyright 2010 American Chemical Society.

was demonstrated. Thus, “smart” nanoparticles can be programmed to control their nanowire assembly.

Smart NPs can exploit magnetic relaxation switching effects, where analytes shuttle NPs between aggregated or dispersed states, changing in the measured relaxation rates. In particular, the clustering of superparamagnetic NPs induces a reduction in the measured  $T_2$ .<sup>83</sup> To give an example, Concanavalin A, a specific lectin against glucose, has been detected and quantified up to microgram levels.<sup>140</sup> Concanavalin A is a multimeric protein, which, when incubated with glucose-derivatized NPs, can induce the agglomeration of the NPs. The concentration of Concanavalin A could be easily monitored by variation in  $T_2$  due to NP clustering. The level of agglomeration is sensitive to glucose density on the surface of NPs. High concentrations decrease agglomeration, presumably due to steric hindrance. Going further, these NPs could also provide information about the quaternary structure of the lectin. It was observed

that the variation of  $T_2$  with increasing Concanavalin A concentration was higher at pH 7 than at pH 4. These changes were attributed to different quaternary structures of Concanavalin A at different pH. For instance, Concanavalin A is a dimer at pH 4 but evolves into a tetramer at pH 7, explaining the higher tendency to agglomerate at higher pH. Beyond biomolecule assays *in vitro*,<sup>83,141,142</sup> magnetic NPs have been used to measure levels of analytes *in vivo*.<sup>143,144</sup> Magnetic NPs have served as platforms for the design of enzyme-activated fluorescent probes.<sup>145–148</sup> Recently, the attachment of DNA-binding fluorochromes to NP surfaces have provided a new approach for the detection of PCR-generated DNA and monitoring the PCR reaction.<sup>149</sup>

Apart from sensing, there are many applications for “smart” NPs in delivery. The primary function of the NPs in this case is as delivery vehicles for attached pharmaceutical agents.<sup>150</sup> Nanoparticles can be designed in such a way that they change their properties depending on local stimuli during delivery.

Changes in properties may involve variations in size, porosity, and binding affinity of the transported pharmaceutical agent. These properties may affect uptake of the NPs by cells/organs, as this is often a size-dependent process, and may also affect the release of the cargo molecules. Frequently used stimuli involve changes in pH and temperature. Responsive microgels, particularly hydrogels, have been studied for use in controlled drug delivery. The interest in these systems is due to their network swelling and shrinking as a function of external stimuli. In addition, their porous structure allows drugs to be loaded into the interior of the microgel network and then released upon temperature- or pH-induced swelling.<sup>151</sup> The size of the microgels can be tuned through synthetic procedures, and their water solubility and biocompatibility make them excellent candidates for biological applications.<sup>152</sup> Furthermore, incorporating NPs that have optical or fluorescent properties into the network of microgels enables tracking of the particles throughout the body.

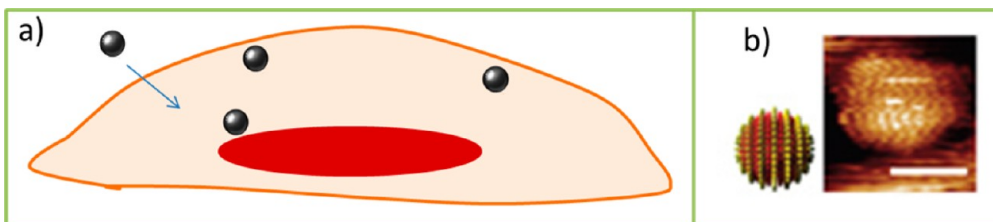


**Figure 7.** (a) Nanoparticles modified with hydrophilic/hydrophobic stripes can directly penetrate the cellular membrane for delivery into the cytosol. (b) Schematic of a striped NP and its corresponding image as recorded with scanning tunneling microscopy. The scale bar corresponds to 5 nm. Image reproduced with permission from ref 162. Copyright 2008 Nature.

The ultimate version of a “smart” NP would involve a complete feedback loop. Such a NP would be capable of acting on the environment (e.g., by heating locally or altering the local pH or concentration of a particular signaling molecule, etc.) and in turn providing a transduction signal (a read-out response) from the environment driven by resonance energy transfer, charge transfer, or other means that enables sensing of molecules, temperature, etc. Read-out would influence the action, whereby feedback loops might be based on interaction with light, temperature, or pH. Although NPs that can be manipulated by these triggers and NP-conjugates that can report on such processes exist, integration of all these elements into a feedback loop is currently beyond our reach. Thus, we continue to work toward “smart” multifunctional NPs that affect their environment *via* specific triggering mechanisms, are sensitive to their surroundings *via* feedback loops, and play increasing roles in sensing and other biological processes.

### Nanoparticles can be designed to be smart.

**Surface-modified nanoparticles can directly reach the cytosol of living cells.** For many *in vitro* delivery applications, one would like NPs that directly reach the cytosol of the cells.<sup>153</sup> However, the cytosol is surrounded by the cellular membrane, which is a protein-enriched lipid double layer. Thus, there are only two principal ways to reach the cytosol. In the first,

NPs can enter the membrane and embed in the bud that is formed and eventually pinch off. This endocytic pathway leaves the NPs encapsulated in membrane vesicles, in endosomes and lysosomes. Thus, to transfer the NPs to the cytosol, they have to escape from the endosomes/lysosomes, which can be achieved, for example, by buffering the acidity in the vesicles.<sup>154</sup> In the second pathway, NPs can directly traverse the cellular membrane *via* dynamically formed pores, which would enable direct entry into the cytosol without the surrounding lipid membrane. Though the first pathway is more common, there are several successful examples of direct entry.

One of the most widely used strategies for the internalization of NPs into cells is the incorporation of cell penetrating peptides (CPPs), such as TAT.<sup>155</sup> The TAT peptide has the property of leaving HIV-infected cells, going through the cell membranes of noninfected cells, and even reaching the cell nucleus. The region used for intracellular transduction is called the protein transduction domain (PTD). For example, Weissleder's group has delivered iron oxide NPs conjugated with TAT into the cell cytoplasm.<sup>156</sup> In addition, if the TAT peptide is further modified with a nuclear localization sequence, it could be used for the delivery of NPs to the cell nucleus. Here, the nuclear pore complex (NPC) provides an “entry door” to the nucleus, while the TAT is a key to open this door. However, the diameter of the NPC opens to a maximum of 30 nm using active transport (or only 9 nm for diffusive transport). This is one of the main problems for delivery

inside the nucleus: cargo sizes must be smaller than the NPC. In fact, gold NPs functionalized with TAT peptides and with an overall size of 5 nm can be driven into a cell nucleus, although 30 nm NPs cannot, mainly due to this size limitation.<sup>157</sup> Many other naturally derived peptides, such as penetratin<sup>158</sup> and transportan,<sup>159</sup> have shown great promise in drug-delivery applications. Although the mechanism used by CPPs to cross cell membranes is unknown, they have been extensively used to transport different types of NPs into cells.<sup>160,161</sup>

Alternatively, one can construct assemblies of NPs that penetrate through the cellular membrane, bypassing endocytosis.<sup>55</sup> The mechanism of such transport is also not well understood. Conceptually, one can speculate that if individual water-soluble NPs behave like proteins (see Figures 1 and 2), assemblies of several NPs can behave like viruses (see Figure 4a–d), which manifest the distinct ability to penetrate cellular membranes with little resistance and to avoid digestion in endosomes. One can also notice that both penetratin and transportan have elongated “corkscrew”-like geometries, which could be replicated in nanoscale inorganic structures and in NP assemblies.

Yet another example involves NPs with striped patterns of hydrophilic and hydrophobic domains on their surfaces. Interactions of this patterned cap with the cell membrane lead to transient poration of the membrane and thus delivery of the NPs directly into the cytosol (see Figure 7).<sup>162</sup> Although the details of the delivery mechanism need

to be investigated, such systems have already been used for transporting cargo into cells.<sup>163</sup>

It is evident from the discussion above that the molecular details of direct transport of NPs into the cytosol are not yet known. One problem is the difficulty in observing incorporation at the molecular level. Typically, the locations of the NPs in the cytosol are determined by transmission electron microscopy<sup>164</sup> or by fluorescence-based immunostaining. Modification of NPs with pH-sensitive fluorophores might help, as location could be determined by reading out the local pH, which differs between the endo/lysosomes and the cytosol.

As a general conclusion, there are several new directions in the field of nanoscience, that is, studies of more complex 1D, 2D, and 3D nanoscale systems in which NPs serve as individual building blocks rather than ideas exploiting the properties of individual NPs. One can also envision more complex properties of individual NPs resulting in adaptable dynamic nanoscale systems even if they contain only one NP. Several fields, such as the synthesis of NPs with excellent size and shape distributions have neared maturity, whereas other fields, such as those involving applications with complex NP assemblies, are still developing. In the context of medical applications of NPs much has been done, and exciting opportunities will appear in the near future, such as early diagnosis of cancer and potential delivery vehicles for targeted therapeutics. However, before the next-generation NPs can reach the clinic, deeper understanding and control over the interface between nanoscience and biology, along with the optimization of the biological performance of the NPs and bioconjugates, remain critical.

**Conflict of Interest:** The authors declare no competing financial interest.

**Acknowledgment.** This article was inspired by reports at the NANAX5 conference held in Fuengirola, Spain, May 7–11, 2012. Parts of this work were funded by DFG PA 794/11-1 (to W.J.P.), ERC-Starting

Grant Nanopuzzle and ARAID (to J.M.F.), and ERC-Advanced Grant PLASMAQUO (to L.M.L.M.). ERC Advanced Investigator grant HYMEM (J.F.) is acknowledged.

## REFERENCES AND NOTES

- Choi, C. L.; Alivisatos, A. P. From Artificial Atoms to Nanocrystal Molecules: Preparation and Properties of More Complex Nanostructures. *Annu. Rev. Phys. Chem.* **2010**, *61*, 369–389.
- Guerrero-Martinez, A.; Grzelczak, M.; Liz-Marzan, L. M. Molecular Thinking for Nanoplasmonic Design. *ACS Nano* **2012**, *6*, 3655–3662.
- Kotov, N. A. Inorganic Nanoparticles as Protein Mimics. *Science* **2010**, *330*, 188–189.
- Vossmeye, T.; Reck, G.; Schulz, B.; Katsikas, L.; Weller, H. Double-Layer Superlattice Structure Built up of  $\text{Cd}_{32}\text{S}_{14}(\text{SCH}_2\text{CH}(\text{OH})\text{CH}_3)_{36}\cdot 4\text{H}_2\text{O}$  Clusters. *J. Am. Chem. Soc.* **1995**, *117*, 12881–12882.
- Rivera Gil, P.; Jimenez de Aberasturi, D.; Wulf, V.; Pelaz, B.; del Pino, P.; Zhao, Y.; de la Fuente, J. M.; Ruiz de Larramendi, I.; Rojo, T.; Liang, X.-J.; et al. The Challenge To Relate the Physicochemical Properties of Colloidal Nanoparticles to Their Cytotoxicity. *Acc. Chem. Res.* **2012**, *10.1021/ar300039j*.
- Dong, A.; Chen, J.; Oh, S. J.; Koh, W.-k.; Xiu, F.; Ye, X.; Ko, D.-K.; Wang, K. L.; Kagan, C. R.; Murray, C. B. Multiscale Periodic Assembly of Striped Nanocrystal Superlattice Films on a Liquid Surface. *Nano Lett.* **2011**, *11*, 841–846.
- Tang, Z.; Kotov, N. A.; Giersig, M. Spontaneous Organization of Single CdTe Nanoparticles into Luminous Nanowires. *Science* **2002**, *297*, 237–240.
- Sinyagin, A. Y.; Belov, A.; Tang, Z.; Kotov, N. A. Monte Carlo Computer Simulation of Chain Formation from Nanoparticles. *J. Phys. Chem. B* **2006**, *110*, 7500–7507.
- Tang, Z.; Zhang, Z.; Wang, Y.; Glotzer, S. C.; Kotov, N. A. Self-Assembly of CdTe Nanocrystals into Free-Floating Sheets. *Science* **2006**, *314*, 274–278.
- Srivastava, S.; Santos, A.; Critchley, K.; Kim, K. S.; Podsiadlo, P.; Sun, K.; Lee, J.; Xu, C.; Lilly, G. D.; Glotzer, S. C.; et al. Light-Controlled Self-Assembly of Semiconductor Nanoparticles into Twisted Ribbons. *Science* **2010**, *327*, 1355–1359.
- Caswell, K. K.; Wilson, J. N.; Bunz, U. H. F.; Murphy, C. J. Preferential End-to-End Assembly of Gold Nanorods by Biotin-Streptavidin Connectors. *J. Am. Chem. Soc.* **2003**, *125*, 13914–13915.
- Nie, Z.; Fava, D.; Rubinstein, M.; Kumacheva, E. "Supramolecular" Assembly of Gold Nanorods End-Terminated with Polymer "Pom-Poms": Effect of Pom-Pom Structure on the Association Modes. *J. Am. Chem. Soc.* **2008**, *130*, 3683–3689.
- Yoo, S. I.; Yang, M.; Brender, J. R.; Subramanian, V.; Sun, K.; Joo, N. E.; Jeong, S. H.; Ramamoorthy, A.; Kotov, N. A. Inhibition of Amyloid Peptide Fibrillation by Inorganic Nanoparticles: Functional Similarities with Proteins. *Angew. Chem., Int. Ed.* **2011**, *50*, 5110–5115.
- Manea, F.; Houillon, F. B.; Pasquato, L.; Scrimin, P. Nanozymes: Gold-Nanoparticle-Based Transphosphorylation Catalysts. *Angew. Chem., Int. Ed.* **2004**, *43*, 6165–6169.
- Mahtab, R.; Harden, H. H.; Murphy, C. J. Temperature- and Salt-Dependent Binding of Long DNA to Protein-Sized Quantum Dots: Thermodynamics of "Inorganic Protein"–DNA Interactions. *J. Am. Chem. Soc.* **2000**, *122*, 14–17.
- Claridge, S. A.; Schwartz, J. J.; Weiss, P. S. Electrons, Photons, and Force: Quantitative Single-Molecule Measurements from Physics to Biology. *ACS Nano* **2011**, *5*, 693–729.
- Rogach, A. L. Fluorescence Energy Transfer in Hybrid Structures of Semiconductor Nanocrystals. *Nano Today* **2011**, *6*, 355–365.
- Chanyawadee, S.; Harley, R. T.; Taylor, D.; Henini, M.; Susha, A. S.; Rogach, A. L.; Lagoudakis, P. G. Efficient Light Harvesting in Hybrid CdTe Nanocrystal/Bulk GaAs P-I-N Photovoltaic Devices. *Appl. Phys. Lett.* **2009**, *94*, 233502.
- Clapp, A. R.; Medintz, I. L.; Mauro, J. M.; Fisher, B. R.; Bawendi, M. G.; Mattossi, H. Fluorescence Resonance Energy Transfer between Quantum Dot Donors and Dye-Labeled Protein Acceptors. *J. Am. Chem. Soc.* **2004**, *126*, 301–310.
- Becker, K.; Rogach, A. L.; Feldmann, J.; Talapin, D. V.; Lupton, J. M. Energetic Disorder Limits Energy Transfer in Semiconductor Nanocrystal–DNA–Dye Conjugates. *Appl. Phys. Lett.* **2009**, *95*, 143101.
- Jiang, G.; Susha, A. S.; Lutich, A. A.; Stefani, F. D.; Feldmann, J.; Rogach, A. L. Cascaded FRET in Conjugated Polymer/Quantum Dot/Dye-Labeled DNA Complexes for DNA Hybridization Detection. *ACS Nano* **2009**, *3*, 4127–4131.
- Rogach, A. L.; Gaponik, N.; Lupton, J. M.; Bertoni, C.; Gallardo, D. E.; Dunn, S.; Li Pira, N.; Paderi, M.; Repetto, P.; Romanov, S. G.; et al. Light-Emitting Diodes with Semiconductor Nanocrystals. *Angew. Chem. Int. Ed.* **2008**, *47*, 6538–6549.
- Gaponik, N.; Hickey, S. G.; Dorfs, D.; Rogach, A. L.; Eychmuller, A. Progress in the Light Emission of Colloidal Semiconductor Nanocrystals. *Small* **2010**, *6*, 1364–1378.
- Rizzo, A.; Li, Y. Q.; Kudera, S.; Della Sala, F.; Zanella, M.; Parak, W. J.; Cingolani, R.; Manna, L.; Gigli, G. Blue Light Emitting Diodes Based on

Fluorescent CdSe/ZnS Nanocrystals. *Appl. Phys. Lett.* **2007**, *90*, 051106.

25. Jasieniak, J.; MacDonald, B. I.; Watkins, S. E.; Mulvaney, P. Solution-Processed Sintered Nanocrystal Solar Cells via Layer-by-Layer Assembly. *Nano Lett.* **2011**, *11*, 2856–2864.

26. Freeman, R.; Liu, X.; Willner, I. Chemiluminescent and Chemiluminescence Resonance Energy Transfer (CRET) Detection of DNA, Metal Ions, and Aptamer/Substrate Complexes Using Hemin/G-Quadruplexes CdSe/ZnS Quantum Dots. *J. Am. Chem. Soc.* **2011**, *133*, 11597–11604.

27. Soenen, S. J.; Rivera Gil, P.; Montenegro, J. M.; Parak, W. J.; De Smedt, S. C.; Braeckmans, K. Cellular Toxicity of Inorganic Nanoparticles: Common Aspects and Guidelines for Improved Nanotoxicity Evaluation. *Nano Today* **2011**, *6*, 446–465.

28. Deen, W. M.; Bridges, C. R.; Brenner, B. M.; Myers, B. D. Heteroporous Model of Glomerular Size Selectivity: Application to Normal and Nephrotic Humans. *Am. J. Physiol.* **1985**, *249*, F374–F389.

29. Pullela, S. R.; Andres, C.; Chen, W.; Xu, C.; Wang, L.; Kotov, N. A. Permeability/Electrolyte Replication of Artificial Glomerular Basement Membranes in Nanoporous Collagen Multilayers. *J. Phys. Chem. Lett.* **2011**, *2*, 2067–2072.

30. Pan, Y.; Neuss, S.; Leifert, A.; Fischler, M.; Wen, F.; Simon, U.; Schmid, G.; Brandau, W.; Jähnchen-Dechent, W. Size-Dependent Cytotoxicity of Gold Nanoparticles. *Small* **2007**, *3*, 1941–1949.

31. Schipper, M. L.; Iyer, G.; Koh, A. L.; Cheng, Z.; Ebenstein, Y.; Aharoni, A.; Keren, S.; Bentolila, L. A.; Li, J. Q.; Rao, J. H.; et al. Particle Size, Surface Coating, and Pegylation Influence the Biodistribution of Quantum Dots in Living Mice. *Small* **2009**, *5*, 126–134.

32. Jähnchen-Dechent, W.; Simon, U. Function Follows Form: Shape Complementarity and Nanoparticle Toxicity. *Nanomedicine (London)* **2008**, *3*, 601–603.

33. De Jong, W. H.; Hagens, W. I.; Kryszteki, P.; Burger, M. C.; Sips, A. J.; Geertsma, R. E. Particle Size-Dependent Organ Distribution of Gold Nanoparticles after Intravenous Administration. *Biomaterials* **2008**, *29*, 1912–1919.

34. Sonavane, G.; Tomoda, K.; Makino, K. Biodistribution of Colloidal Gold Nanoparticles after Intravenous Administration: Effect of Particle Size. *Colloids Surf. B* **2008**, *66*, 274–280.

35. Almeida, J. P.; Chen, A. L.; Foster, A.; Drezek, R. In Vivo Biodistribution of Nanoparticles. *Nanomedicine (London)* **2011**, *6*, 815–835.

36. Cho, W. S.; Cho, M.; Jeong, J.; Choi, M.; Han, B. S.; Shin, H. S.; Hong, J.; Chung, B. H.; Jeong, J.; Cho, M. H. Size-Dependent Tissue Kinetics of Peg-Coated Gold Nanoparticles. *Toxicol. Appl. Pharmacol.* **2010**, *245*, 116–123.

37. Choi, H. S.; Liu, W.; Misra, P.; Tanaka, E.; Zimmer, J. P.; Itty Ipe, B.; Bawendi, M. G.; Frangioni, J. V. Renal Clearance of Quantum Dots. *Nat. Biotechnol.* **2007**, *25*, 1165–1170.

38. Chomoucka, J.; Drbohlavova, J.; Huska, D.; Adam, V.; Kizek, R.; Hubalek, J. Magnetic Nanoparticles and Targeted Drug Delivering. *Pharmacol. Res.* **2010**, *62*, 144–149.

39. Schipper, M. L.; Cheng, Z.; Lee, S.-W.; Bentolila, L. A.; Iyer, G.; Rao, J.; Chen, X.; Wu, A. M.; Weiss, S.; Gambhir, S. S. MicroPET-Based Biodistribution of Quantum Dots in Living Mice. *J. Nucl. Med.* **2007**, *48*, 1511–1518.

40. Ballou, B.; Lagerholm, B. C.; Ernst, L. A.; Bruchez, M. P.; Waggoner, A. S. Noninvasive Imaging of Quantum Dots in Mice. *Bioconjugate Chem.* **2004**, *15*, 79–86.

41. Hirn, S.; Semmler-Behnke, M.; Schlehr, C.; Wenk, A.; Lipka, J.; Schaffler, M.; Takenaka, S.; Moller, W.; Schmid, G.; Simon, U.; et al. Particle Size-Dependent and Surface Charge-Dependent Biodistribution of Gold Nanoparticles after Intravenous Administration. *Eur. J. Pharm. Biopharm.* **2011**, *77*, 407–416.

42. Xia, Y.; Nguyen, T. D.; Yang, M.; Lee, B.; Santos, A.; Podsiadlo, P.; Tang, Z.; Glotzer, S. C.; Kotov, N. A. Self-Assembly of Self-Limiting Monodisperse Supraparticles from Polydisperse Nanoparticles. *Nat. Nanotechnol.* **2011**, *6*, 580–587.

43. Wang, L.; Xu, L.; Kuang, H.; Xu, C.; Kotov, N. A. Dynamic Nanoparticle Assemblies. *Acc. Chem. Res.* **2012**, *45*, 10.1021/ar200305f.

44. Sperling, R. A.; Rivera Gil, P.; Zhang, F.; Zanella, M.; Parak, W. J. Biological Applications of Gold Nanoparticles. *Chem. Soc. Rev.* **2008**, *37*, 1896–1908.

45. Colombo, M.; Carregal-Romero, S.; Casula, M. F.; Gutiérrez, L.; Morales, M. P.; Böhm, I. B.; Heverhagen, J. T.; Prosperi, D.; Parak, W. J. Biological Applications of Magnetic Nanoparticles. *Chem. Soc. Rev.* **2012**, *41*, 4306–4334.

46. De, M.; Gosh, P. S.; Rotello, V. M. Applications of Nanoparticles in Biology. *Adv. Mater.* **2008**, *20*, 4225–4241.

47. Grzelczak, M.; Vermant, J.; Furst, E. M.; Liz-Marzan, L. M. Directed Self-Assembly of Nanoparticles. *ACS Nano* **2010**, *4*, 3591–3605.

48. Romo-Herrera, J. M.; Alvarez-Puebla, R. A.; Liz-Marzan, L. M. Controlled Assembly of Plasmonic Colloidal Nanoparticle Clusters. *Nanoscale* **2010**, *3*, 1304–1315.

49. Karg, M. Multifunctional Inorganic/Organic Hybrid Microgels. *Colloid Polym. Sci.* **2012**, *280*, 673–688.

50. Liz-Marzán, L. M.; Mulvaney, P. The Assembly of Coated Nanocrystals. *J. Phys. Chem. B* **2003**, *107*, 7312–7326.

51. Mohanan, J. L.; Arachchige, I. U.; Brock, S. L. Porous Semiconductor Chalcogenide Aerogels. *Science* **2005**, *307*, 397–400.

52. Yang, M.; Sun, K.; Kotov, N. A. Formation and Assembly-Disassembly Processes of ZnO Hexagonal Pyramids Driven by Dipolar and Excluded Volume Interactions. *J. Am. Chem. Soc.* **2010**, *132*, 1860–1872.

53. Jaber, S.; Karg, M.; Morfa, A.; Mulvaney, P. 2D Assembly of Gold–PNIPAM Core–Shell Nanocrystals. *Phys. Chem. Chem. Phys.* **2011**, *13*, 5576–5578.

54. Karg, M.; Hellweg, T.; Mulvaney, P. Self-Assembly of Tunable Nanocrystal Superlattices Using Poly-(NIPAM) Spacers. *Adv. Funct. Mater.* **2011**, *21*, 4668–4676.

55. Xu, L.; Kuang, H.; Xu, C.; Ma, W.; Wang, L.; Kotov, N. A. Regiospecific Plasmonic Assemblies for *in Situ* Raman Spectroscopy in Live Cells. *J. Am. Chem. Soc.* **2012**, *134*, 1699–1709.

56. Wang, L. B.; Zhu, Y. Y.; Xu, L. G.; Chen, W.; Kuang, H.; Liu, L. Q.; Agarwal, A.; Xu, C. L.; Kotov, N. A. Side-by-Side and End-to-End Gold Nanorod Assemblies for Environmental Toxin Sensing. *Angew. Chem., Int. Ed.* **2010**, *49*, 5472–5475.

57. Shenton, W.; Davis, S. A.; Mann, S. Directed Self-Assembly of Nanoparticles into Macroscopic Materials Using Antibody-Antigen Recognition. *Adv. Mater.* **2001**, *11*, 449–452.

58. Sleytr, U. B.; Messner, P.; Pum, D.; Sara, M. Crystalline Bacterial Cell Surface Layers (S Layers): From Supramolecular Cell Structure to Biomimetics and Nanotechnology. *Angew. Chem., Int. Ed.* **1999**, *38*, 1035–1054.

59. Györvary, E.; Schroedter, A.; Talaipin, D. V.; Weller, H.; Pum, D.; Sleytr, U. B. Formation of Nanoparticle Arrays on S-Layer Protein Lattices. *J. Nanosci. Nanotechnol.* **2004**, *4*, 115–120.

60. McMillan, R. A.; Paavola, C. D.; Howard, J.; Chan, S. L.; Zaluzec, N. J.; Trent, J. D. Ordered Nanoparticle Arrays Formed on Engineered Chaperonin Protein Templates. *Nat. Mater.* **2002**, *1*, 247–252.

61. Winfree, E.; Liu, F.; Wenzler, L. A.; Seeman, N. C. Design and Self-Assembly of Two-Dimensional DNA Crystals. *Nature* **1998**, *394*, 539–544.

62. Le, J. D.; Pinto, Y.; Seeman, N. C.; Musier-Forsyth, K.; Taton, T. A.; Kiehl, R. A. DNA-Templated Self-Assembly of Metallic Nanocomponent Arrays on a Surface. *Nano Lett.* **2004**, *4*, 2343–2347.

63. Zheng, J.; Constantinou, P. E.; Micheel, C.; Alivisatos, A. P.; Kiehl, R. A.; Seeman, N. C. Two-Dimensional Nanoparticle Arrays Show the Organizational Power of Robust DNA Motifs. *Nano Lett.* **2006**, *6*, 1502–1504.

64. Wilner, O. I.; Orbach, R.; Henning, A.; Teller, C.; Yehezkel, O.; Mertig, M.; Harries, D.; Willner, I. Self-Assembly of DNA Nanotubes with Controllable Diameters. *Nat. Commun.* **2011**, *2*, 540.

65. Rothemund, P. W. K. Folding DNA To Create Nanoscale Shapes and Patterns. *Nature* **2006**, *440*, 297–302.

66. Kuzyk, A.; Schreiber, R.; Fan, Z. Y.; Pardatscher, G.; Roller, E. M.; Hoge, A.; Simmel, F. C.; Govorov, A. O.; Liedl, T. DNA-Based Self-Assembly of Chiral Plasmonic Nanostructures with Tailored Optical Response. *Nature* **2012**, *483*, 311–314.

67. Acuna, G. P.; Bucher, M.; Stein, I. H.; Steinhauer, C.; Kuzyk, A.; Holzmeister, P.; Schreiber, R.; Moroz, A.; Stefani, F. D.; Liedl, T.; et al. Distance Dependence of Single-Fluorophore Quenching by Gold Nanoparticles Studied on DNA Origami. *ACS Nano* **2012**, *6*, 3189–3195.

68. Klar, T. A.; Franzl, T.; Rogach, A. L.; Feldmann, J. Super-Efficient Exciton Funneling in Layer-by-Layer Semiconductor Nanocrystal Structures. *Adv. Mater.* **2005**, *17*, 769–773.

69. Kagan, C. R.; Murray, C. B.; Nirmal, M.; Bawendi, M. G. Electronic Energy Transfer in CdSe Quantum Dot Solids. *Phys. Rev. Lett.* **1996**, *76*, 1517–1520.

70. Crooker, S. A.; Hollingsworth, J. A.; Tretiak, S.; Klimov, V. I. Spectrally Resolved Dynamics of Energy Transfer in Quantum-Dot Assemblies: Towards Engineered Energy Flows in Artificial Materials. *Phys. Rev. Lett.* **2002**, *89*, 186802.

71. Kovalenko, M. V.; Scheele, M.; Talapin, D. V. Colloidal Nanocrystals with Molecular Metal Chalcogenide Surface Ligands. *Science* **2009**, *324*, 1417–1420.

72. Nag, A.; Kovalenko, M. V.; Lee, J.-S.; Liu, W.; Spokoyny, B.; Talapin, D. V. Metal-Free Inorganic Ligands for Colloidal Nanocrystals:  $S^{2-}$ ,  $HS^-$ ,  $Se^{2-}$ ,  $HSe^-$ ,  $Te^{2-}$ ,  $HTe^-$ ,  $TeS_3^{2-}$ ,  $OH^-$  and  $NH_2^-$  as Surface Ligands. *J. Am. Chem. Soc.* **2011**, *133*, 10612–10620.

73. Fafarman, A. T.; Koh, W.-k.; Diroll, B. T.; Kim, D. K.; Ko, D.-K.; Oh, S. J.; Ye, X.; Doan-Nguyen, V.; Crump, M. R.; Reifsnyder, D. C.; et al. Thiocyanate-Capped Nanocrystal Colloids: Vibrational Reporter of Surface Chemistry and Solution-Based Route to Enhanced Coupling in Nanocrystal Solids. *J. Am. Chem. Soc.* **2011**, *133*, 15753–15761.

74. Lee, J.-S.; Kovalenko, M. V.; Huang, J.; Chung, D. S.; Talapin, D. V. Band-like Transport, High Electron Mobility and High Photoconductivity in All-Inorganic Nanocrystal Arrays. *Nat. Nanotechnol.* **2011**, *6*, 348–352.

75. Choi, J.-H.; Fafarman, A. T.; Oh, S. J.; Ko, D.-K.; Kim, D. K.; Diroll, B. T.; Muramoto, S.; Gillen, J. G.; Murray, C. B.; Kagan, C. R. Bandlike Transport in Strongly Coupled and Doped Quantum Dot Solids: A Route to High-Performance Thin-Film Electronics. *Nano Lett.* **2012**, *12*, 2631–2638.

76. Sanchot, A.; Baffou, G.; Marty, R.; Arbouet, A.; Quidant, R.; Girard, C.; Dujardin, E. Plasmonic Nanoparticle Networks for Light and Heat Concentration. *ACS Nano* **2012**, *6*, 3434–3440.

77. Hrelescu, C.; Stehr, J.; Ringler, M.; Sperling, R. A.; Parak, W. J.; Klar, T. A.; Feldmann, J. DNA Melting in Gold Nanostove Clusters. *J. Phys. Chem. C* **2010**, *114*, 7401–7411.

78. Shimizu, K. T.; Woo, W. K.; Fisher, B. R.; Eisler, H. J.; Bawendi, M. G. Surface-Enhanced Emission from Single Semiconductor Nanocrystals. *Phys. Rev. Lett.* **2002**, *89*, 117401.

79. Okamoto, K.; Vyawahare, S.; Scherer, A. Surface-Plasmon Enhanced Bright Emission from CdSe Quantum-Dot Nanocrystals. *J. Opt. Soc. Am. B* **2006**, *23*, 1674–1678.

80. Alvarez-Puebla, R.; Liz-Marzan, L. M.; de Abajo, F. J. G. Light Concentration at the Nanometer Scale. *J. Phys. Chem. Lett.* **2010**, *1*, 2428–2434.

81. Sanchez-Iglesias, A.; Aldeanueva-Potel, P.; Ni, W. H.; Perez-Juste, J.; Pastoriza-Santos, I.; Alvarez-Puebla, R. A.; Mbenkum, B. N.; Liz-Marzan, L. M. Chemical Seeded Growth of Ag Nanoparticle Arrays and Their Application as Reproducible SERS Substrates. *Nano Today* **2010**, *5*, 21–27.

82. Abbasi, A. Z.; Gutierrez, L.; del Mercato, L. L.; Herranz, F.; Chubykalo-Fesenko, O.; Veintemillas-Verdaguer, S.; Parak, W. J.; Morales, M. P.; Gonzalez, J. M.; Hernando, A.; et al. Magnetic Capsules for NMR Imaging: Effect of Magnetic Nanoparticles Spatial Distribution and Aggregation. *J. Phys. Chem. C* **2011**, *115*, 6257–6264.

83. Perez, J. M.; Josephson, L.; Weissleder, R. Use of Magnetic Nanoparticles as Nanosensors To Probe for Molecular Interactions. *ChemBioChem* **2004**, *5*, 261–264.

84. Schaaff, T. G.; Whetten, R. L. Giant Gold-Glutathione Cluster Compounds: Intense Optical Activity in Metal-Based Transitions. *J. Phys. Chem. B* **2000**, *104*, 2630–1641.

85. Mastroianni, A. J.; Claridge, S. A.; Alivisatos, A. P. Pyramidal and Chiral Groupings of Gold Nanocrystals Assembled Using DNA Scaffolds. *J. Am. Chem. Soc.* **2009**, *131*, 8455–8459.

86. Chen, W.; Bian, A.; Agarwal, A.; Liu, L.; Shen, H.; Wang, L.; Xu, C.; Kotov, N. A. Nanoparticle Superstructures Made by Polymerase Chain Reaction: Collective Interactions of Nanoparticles and a New Principle for Chiral Materials. *Nano Lett.* **2009**, *9*, 2153–2159.

87. Lilly, G. D.; Agarwal, A.; Srivastava, S.; Kotov, N. A. Helical Assemblies of Gold Nanoparticles. *Small* **2011**, *7*, 2004–2009.

88. Guerrero-Martinez, A.; Auguie, B.; Alonso-Gomez, J. L.; Dzolic, Z.; Gomez-Grana, S.; Zinic, M.; Cid, M. M.; Liz-Marzan, L. M. Intense Optical Activity from Three-Dimensional Chiral Ordering of Plasmonic Nanoantennas. *Angew. Chem., Int. Ed.* **2011**, *50*, 5499–5503.

89. Guerrero-Martinez, A.; Alonso-Gomez, J. L.; Auguie, B.; Cid, M. M.; Liz-Marzan, L. M. From Individual to Collective Chirality in Metal Nanoparticles. *Nano Today* **2011**, *6*, 381–400.

90. Zhou, C.; Tsai, T. H.; Adler, D. C.; Lee, H. C.; Cohen, D. W.; Mondelblatt, A.; Wang, Y. H.; Connolly, J. L.; Fujimoto, J. G. Photothermal Optical Coherence Tomography in *ex Vivo* Human Breast Tissues Using Gold Nanoshells. *Opt. Lett.* **2010**, *35*, 700–702.

91. Claridge, S. A.; Castleman, A. W.; Khanna, S. N.; Murray, C. B.; Sen, A.; Weiss, P. S. Cluster-Assembled Materials. *ACS Nano* **2009**, *3*, 244–255.

92. Qian, M.; Reber, A. C.; Ugrinov, A.; Chaki, N. K.; Mandal, S.; Saavedra, H. c. M.; Khanna, S. N.; Sen, A.; Weiss, P. S. Cluster-Assembled Materials: Toward Nanomaterials with Precise Control over Properties. *ACS Nano* **2010**, *4*, 235–240.

93. Chaki, N. K.; Mandal, S.; Reber, A. C.; Qian, M.; Saavedra, H. M.; Weiss, P. S.; Khanna, S. N.; Sen, A. Controlling Band Gap Energies in Cluster-Assembled Ionic Solids through Internal Electric Fields. *ACS Nano* **2010**, *4*, 5813–5818.

94. Klein, D. L.; Roth, R.; Lim, A. K. L.; Alivisatos, A. P.; McEuen, P. L. A Single-Electron Transistor Made from a Cadmium Selenide Nanocrystal. *Nature* **1997**, *389*, 699–701.

95. Weiss, P. S.; Eigler, D. M. What Is Underneath? Moving Atoms and Molecules To Find out, in Nano-sources and Manipulations of Atoms under High Fields and Temperatures: Applications. In *NATO ASI Series E: Applied Sciences*, Thien Binh, V., Garcia, N., Dransfeld, K., Eds.; Kluwer Academic: Dordrecht, Germany1993; Vol. 235, pp 213–217.

96. Smalley, R. E. Of Chemistry, Love and Nanobots. *Sci. Am.* **2001**, *76*–77.

97. Eigler, D. M.; Schweizer, E. K. Positioning Single Atoms with a Scanning Tunneling Microscope. *Nature* **1990**, *344*, 524–526.

98. Bartels, L.; Meyer, G.; Rieder, K. H. Controlled Vertical Manipulation of Single Co Molecules with the Scanning Tunneling Microscope: A Route to Chemical Contrast. *App. Phys. Lett.* **1997**, *71*, 213–215.

99. Puchner, E. M.; Kufer, S. K.; Strackharn, M.; Stahl, S. W.; Gaub, H. E. Nanoparticle Self-Assembly on a DNA-Scaffold Written by Single-Molecule

Cut-and-Paste. *Nano Lett.* **2008**, *8*, 3692–3695.

100. Kufer, S. K.; Puchner, E. M.; Gumpf, H.; Liedl, T.; Gaub, H. E. Single-Molecule Cut-and-Paste Surface Assembly. *Science* **2008**, *319*, 594–596.

101. Urban, A. S.; Lutich, A. A.; Stefani, F. D.; Feldmann, J. Laser Printing Single Gold Nanoparticles. *Nano Lett.* **2010**, *10*, 4794–4798.

102. Nedev, S.; Urban, A. S.; Lutich, A. A.; Feldmann, J. Optical Force Stamping Lithography. *Nano Lett.* **2011**, *11*, 5066–5070.

103. Mingardon, F.; Chanal, A.; Lopez-Contreras, A. M.; Dray, C.; Bayer, E. A.; Fierobe, H. P. Incorporation of Fungal Cellulases in Bacterial Minicellulosomes Yields Viable, Synergistically Acting Cellulolytic Complexes. *Appl. Environ. Microbiol.* **2007**, *73*, 3822–3832.

104. Hetsch, F.; Xu, X.; Wang, H.; Kersha, S. V.; Rogach, A. L. Semiconductor Nanocrystal Quantum Dots as Solar Cell Components and Photosensitizers: Material, Charge Transfer, and Separation Aspects of Some Device Topologies. *J. Phys. Chem. Lett.* **2011**, *2*, 1879–1887.

105. Giménez, S.; Rogach, A. L.; Lutich, A. A.; Gross, D.; Poeschl, A.; Susha, A. S.; Mora-Seró, I.; Lana-Villarreal, T.; Bisquert, J. Energy Transfer versus Charge Separation in Hybrid Systems of Semiconductor Quantum Dots and Ru-Dyes as Potential Co-Sensitizers of  $\text{TiO}_2$ -Based Solar Cells. *J. Appl. Phys.* **2011**, *110*, 014314.

106. Lutich, A. A.; Jiang, G.; Susha, A. S.; Rogach, A. L.; Stefani, F. D.; Feldmann, J. Energy Transfer versus Charge Separation in Type-II Hybrid Organic–Inorganic Nanocomposites. *Nano Lett.* **2009**, *9*, 2636–2640.

107. Chen, C.-C.; Dou, L.; Zhu, R.; Chung, C.-H.; Song, T.-B.; Zheng, Y. B.; Hawks, S.; Li, G.; Weiss, P. S.; Yang, Y. Visibly Transparent Polymer Solar Cells Produced by Solution Processing. *ACS Nano* **2012**, *6*, 7185–7190.

108. Yaacobi-Gross, N.; Garphunkin, N.; Solomesch, O.; Vaneski, A.; Susha, A. S.; Rogach, A. L.; Tessler, N. Combining Ligand-Induced Quantum-Confined Stark Effect with Type II Heterojunction Bilayer Structure in CdTe and CdSe Nanocrystal-Based Solar Cells. *ACS Nano* **2012**, *6*, 3128–3133.

109. Pellegrino, T.; Kudera, S.; Liedl, T.; Javier, A. M.; Manna, L.; Parak, W. J. On the Development of Colloidal Nanoparticles Towards Multifunctional Structures and Their Possible Use for Biological Applications. *Small* **2005**, *1*, 48–63.

110. Wu, M. X.; Liu, H.; Liu, J.; Haley, K. N.; Treadway, J. A.; Larson, J. P.; Ge, N.; Peale, F.; Bruchez, M. P. Immunofluorescent Labeling of Cancer Marker Her2 and Other Cellular Targets with Semiconductor Quantum Dots. *Nat. Biotechnol.* **2003**, *21*, 41–46.

111. Pellegrino, T.; Manna, L.; Kudera, S.; Liedl, T.; Koktysh, D.; Rogach, A. L.; Keller, S.; Rädler, J.; Natile, G.; Parak, W. J. Hydrophobic Nanocrystals Coated with an Amphiphilic Polymer Shell: A General Route to Water Soluble Nanocrystals. *Nano Lett.* **2004**, *4*, 703–707.

112. Lees, E. E.; Nguyen, T. L.; Clayton, A. H.; Mulvaney, P. The Preparation of Colloidally Stable, Water-Soluble, Biocompatible, Semiconductor Nanocrystals with a Small Hydrodynamic Diameter. *ACS Nano* **2009**, *3*, 1121–1128.

113. Tan, S. J.; Jana, N. R.; Gao, S.; Patra, P. K.; Ying, J. Y. Surface-Ligand-Dependent Cellular Interaction, Subcellular Localization, and Cytotoxicity of Polymer-Coated Quantum Dots. *Chem. Mater.* **2010**, *22*, 2239–2247.

114. Zhang, F.; Lees, E.; Amin, F.; Rivera Gil, P.; Yang, F.; Mulvaney, P.; Parak, W. J. Polymer-Coated Nanoparticles: A Universal Tool for Biolabelling Experiments. *Small* **2011**, *7*, 3113–3127.

115. Gao, X.; Cui, Y.; Levenson, R. M.; Chung, L. W. K.; Nie, S. In Vivo Cancer Targeting and Imaging with Semiconductor Quantum Dots. *Nat. Biotechnol.* **2004**, *22*, 969–976.

116. Chan, W. C. W.; Nie, S. Quantum Dot Bioconjugates for Ultrasensitive Nonisotopic Detection. *Science* **1998**, *281*, 2016–2018.

117. Liu, W. H.; Choi, H. S.; Zimmer, J. P.; Tanaka, E.; Frangioni, J. V.; Bawendi, M. Compact Cysteine-Coated CdSe/ZnCdS Quantum Dots for *in Vivo* Applications. *J. Am. Chem. Soc.* **2007**, *129*, 14530–14531.

118. Susumu, K.; Uyeda, H. T.; Medintz, I. L.; Pons, T.; Delehantry, J. B.; Mattooui, H. Enhancing the Stability and Biological Functionalities of Quantum Dots *via* Compact Multifunctional Ligands. *J. Am. Chem. Soc.* **2007**, *129*, 13987–13996.

119. Liu, W.; Howarth, M.; Greytak, A. B.; Zheng, Y.; Nocera, D. G.; Ting, A. Y.; Bawendi, M. G. Compact Biocompatible Quantum Dots Functionalized for Cellular Imaging. *J. Am. Chem. Soc.* **2008**, *130*, 1274–1284.

120. Wu, H.; Zhu, H.; Zhuang, J.; Yang, S.; Liu, C.; Cao, Y. C. Water-Soluble Nanocrystals through Dual-Interaction Ligands. *Angew. Chem., Int. Ed.* **2008**, *47*, 3730–3734.

121. Susumu, K.; Oh, E.; Delehantry, J. B.; Blanco-Canosa, J. B.; Johnson, B. J.; Jain, V.; Hervey, W. J.; Algar, W. R.; Boeneman, K.; Dawson, P. E.; et al. Multifunctional Compact Zwitterionic Ligands for Preparing Robust Biocompatible Semiconductor Quantum Dots and Gold Nanoparticles. *J. Am. Chem. Soc.* **2011**, *133*, 9480–9496.

122. Yildiz, I.; McCaughan, B.; Cruickshank, S. F.; Callan, J. F.; Raymo, F. M. Biocompatible CdSe–ZnS Core–Shell Quantum Dots Coated with Hydrophilic Polythiols. *Langmuir* **2009**, *25*, 7090–7096.

123. Muro, E.; Pons, T.; Lequeux, N.; Fragola, A.; Sanson, N.; Lenkei, Z.; Dubertret, B. Small and Stable Sulfobetaine Zwitterionic Quantum Dots for Functional Live-Cell Imaging. *J. Am. Chem. Soc.* **2010**, *132*, 4556–4557.

124. Mitchell, G. P.; Mirkin, C. A.; Letsinger, R. L. Programmed Assembly of DNA Functionalized Quantum Dots. *J. Am. Chem. Soc.* **1999**, *121*, 8122–8123.

125. Wang, Y. A.; Li, J. J.; Chen, H.; Peng, X. Stabilization of Inorganic Nanocrystals by Organic Dendrons. *J. Am. Chem. Soc.* **2002**, *124*, 2293–2298.

126. Mattooui, H.; Palui, G.; Na, H. B. Luminescent Quantum Dots as Platforms for Probing *in Vitro* and *In Vivo* Biological Processes. *Adv. Drug Delivery Rev.* **2012**, *64*, 138–166.

127. Wang, Q.; Mynar, J. L.; Yoshida, M.; Lee, E.; Lee, M.; Okuro, K.; Kinbara, K.; Aida, T. High-Water-Content Mouldable Hydrogels by Mixing Clay and a Dendritic Molecular Binder. *Nature* **2010**, *463*, 339–343.

128. Wu, X.; Bruchez, M. P. Labeling Cellular Targets with Semiconductor Quantum Dot Conjugates. *Methods. Cell. Biol.* **2004**, *75*, 171–183.

129. Soltesz, E. G.; Kim, S.; Laurence, R. G.; DeGrand, A. M.; Parungo, C. P.; Dor, D. M.; Cohn, L. H.; Bawendi, M. G.; Frangioni, J. V.; Mihaljevic, T. Intraoperative Sentinel Lymph Node Mapping of the Lung Using Near-Infrared Fluorescent Quantum Dots. *Ann. Thorac. Surg.* **2005**, *79*, 269–277.

130. Courty, S.; Luccardini, C.; Bellaiche, Y.; Cappello, G.; Dahan, M. Tracking Individual Kinesin Motors in Living Cells Using Single Quantum-Dot Imaging. *Nano Lett.* **2006**, *6*, 1491–1495.

131. Snee, P. T.; Somers, R. C.; Nair, G.; Zimmer, J. P.; Bawendi, M. G.; Nocera, D. G. A Ratiometric CdSe/ZnS Nanocrystal pH Sensor. *J. Am. Chem. Soc.* **2006**, *128*, 13320–13321.

132. Wang, X.; Boschetti, C.; Ruedas-Rama, M. J.; Tunnacliffe, A.; Hall, E. A. H. Ratiometric pH-Dot ANSors. *Analyst* **2010**, *135*, 1585–1591.

133. Medintz, I. L.; Stewart, M. H.; Trammell, S. A.; Susumu, K.; Delehantry, J. B.; Mei, B. C.; Melinger, J. S.; Blanco-Canosa, J. B.; Dawson, P. E.; Mattooui, H. Quantum-Dot/Dopamine Bioconjugates Function as Redox Coupled Assemblies for *in Vitro* and Intracellular pH Sensing. *Nat. Mater.* **2010**, *9*, 676–684.

134. Ji, X.; Palui, G.; Avellini, T.; Na, H. B.; Yi, C.; Knappenberger, K. L., Jr.; Mattooui, H. On the pH-Dependent Quenching of Quantum Dot Photoluminescence by Redox Active Dopamine. *J. Am. Chem. Soc.* **2012**, *134*, 6006–6017.

135. Freeman, R.; Gill, R.; Shweky, I.; Kotler, M.; Banin, U.; Willner, I. Biosensing and Probing of Intracellular Metabolic Pathways by NADH-Sensitive Quantum Dots. *Angew. Chem., Int. Ed.* **2009**, *48*, 309–313.

136. Ruedas-Rama, M. J.; Hall, E. A. H. Analytical Nanosphere Sensors Using Quantum Dot-Enzyme Conjugates for Urea and Creatinine. *Anal. Chem.* **2010**, *82*, 9043–9049.

137. Zayats, M.; Baron, R.; Popov, I.; Willner, I. Biocatalytic Growth of Au Nanoparticles: From Mechanistic Aspects to Biosensors Design. *Nano Lett.* **2005**, *5*, 21–25.

138. Xiao, Y.; Pavlov, V.; Levine, S.; Niazov, T.; Markovitch, G.; Willner, I. Catalytic Growth of Au Nanoparticles by NAD(P)H Cofactors: Optical Sensors for NAD(P)<sup>+</sup>-Dependent Biocatalyzed Transformations. *Angew. Chem., Int. Ed.* **2004**, *43*, 4519–4522.

139. Basnar, B.; Weizmann, Y.; Cheglakov, Z.; Willner, I. Synthesis of Nanowires Using Dip-Pen Nanolithography and Biocatalytic Inks. *Adv. Mater.* **2006**, *18*, 713–718.

140. Moros, M.; Pelaz, B.; Lopez-Larrubia, P.; Garcia-Martin, M. L.; Grau, V.; de la Fuente, J. M. Engineering Bio-functional Magnetic Nanoparticles for Biotechnological Applications. *Nanoscale* **2010**, *2*, 1746–1755.

141. Josephson, L.; Perez, J. M.; Weissleder, R. Magnetic Nanosensors for the Detection of Oligonucleotide Sequences. *Angew. Chem., Int. Ed.* **2001**, *40*, 3204–3206.

142. Perez, J. M.; O'Loughlin, T.; Simeone, F. J.; Weissleder, R.; Josephson, L. DNA-Based Magnetic Nanoparticle Assembly Acts as a Magnetic Relaxation Nanoswitch Allowing Screening of DNA-Cleaving Agents. *J. Am. Chem. Soc.* **2002**, *124*, 2856–2857.

143. Atanasijevic, T.; Shusteff, M.; Fam, P.; Jasanoff, A. Calcium-Sensitive MRI Contrast Agents Based on Superparamagnetic Iron Oxide Nanoparticles and Calmodulin. *Proc. Natl. Acad. Sci. U.S.A.* **2006**, *103*, 14707–14712.

144. Shapiro, M. G.; Szablowski, J. O.; Langer, R.; Jasanoff, A. Protein Nanoparticles Engineered to Sense Kinase Activity in MRI. *J. Am. Chem. Soc.* **2009**, *131*, 2484–2486.

145. Josephson, L.; Kircher, M. F.; Mahmood, U.; Tang, Y.; Weissleder, R. Near-Infrared Fluorescent Nanoparticles as Combined MR/Optical Imaging Probes. *Bioconjugate Chem.* **2002**, *13*, 554–560.

146. Josephson, L.; Mahmood, U.; Wunderbaldinger, P.; Tang, Y.; Weissleder, R. Pan and Sentinel Lymph Node Visualization Using a Near-Infrared Fluorescent Probe. *Mol. Imaging* **2003**, *2*, 18–23.

147. Kircher, M. F.; Josephson, L.; Weissleder, R. Ratio Imaging of Enzyme Activity Using Dual Wavelength Optical Reporters. *Mol. Imaging* **2002**, *1*, 89–95.

148. Kircher, M. F.; Weissleder, R.; Josephson, L. A Dual Fluorochrome Probe for Imaging Proteases. *Bioconjugate Chem.* **2004**, *15*, 242–248.

149. Alcantara, D.; Guo, Y.; Yuan, H.; Goergen, C. J.; Chen, H. H.; Cho, H.; Sosnovik, D. E.; Josephson, L. Fluorochrome-Functionalized Magnetic Nanoparticles for High-Sensitivity Monitoring of the Polymerase Chain Reaction by Magnetic Resonance. *Angew. Chem., Int. Ed.* **2012**, *51*, 6904–6907.

150. Farokhzad, O. C.; Langer, R. Impact of Nanotechnology on Drug Delivery. *ACS Nano* **2009**, *3*, 16–20.

151. Das, M.; Zhang, H.; Kumacheva, E. Microgels: Old Materials with New Applications. *Annu. Rev. Mater. Res.* **2006**, *36*, 117–142.

152. Hoare, T. R.; Kohane, D. S. Hydrogels in Drug Delivery: Progress and Challenges. *Polymer* **2008**, *49*, 1993–2007.

153. Luccardini, C.; Yakovlev, A.; Gaillard, S.; Hoff, M. v. t.; Alberola, A. P.; Mallet, J.-M.; Parak, W. J.; Feltz, A.; Oheim, M. Getting across the Plasma Membrane and Beyond: Intracellular Uses of Colloidal Semiconductor Nanocrystals. *J. Biomed. Biotechnol.* **2007**, *2007*, 68963.

154. Wagner, E. Polymers for siRNA Delivery: Inspired by Viruses To Be Targeted, Dynamic, and Precise. *Acc. Chem. Res.* **2012**, *5*, 1005–1013.

155. Vives, E. Present and Future of Cell-Penetrating Peptide Mediated Delivery Systems: "Is the Trojan Horse Too Wild To Go Only to Troy?" *J. Controlled Release* **2005**, *109*, 77–85.

156. Josephson, L.; Tung, C.-H.; Moore, A.; Weissleder, R. High-Efficiency Intracellular Magnetic Labeling with Novel Superparamagnetic-TAT Peptide Conjugates. *Bioconjugate Chem.* **1999**, *10*, 186–191.

157. Berry, C. C.; de la Fuente, J. M.; Mullin, M.; Chu, S. W. L.; Curtis, A. S. G. Nuclear Localization of HIV-1 Tat Functionalized Gold Nanoparticles. *IEEE Trans. Nanobiosci.* **2007**, *6*, 262–269.

158. Child, H. W.; Del Pino, P. A.; De La Fuente, J. M.; Hursthouse, A. S.; Stirling, D.; Mullen, M.; McPhee, G. M.; Nixon, C.; Jayawarna, V.; Berry, C. C. Working Together: The Combined Application of a Magnetic Field and Penetratin for the Delivery of Magnetic Nanoparticles to Cells in 3D. *ACS Nano* **2011**, *5*, 7910–7919.

159. Lundin, P.; Johansson, H.; Guterstam, P.; Holm, T.; Hansen, M.; Langel, U.; El Andaloussi, S. Distinct Uptake Routes of Cell-Penetrating Peptide Conjugates. *Bioconjugate Chem.* **2008**, *19*, 2535–2542.

160. de la Fuente, J. M.; Fandel, M.; Berry, C. C.; Riehle, M.; Cronin, L.; Aitchison, G.; Curtis, A. S. Quantum Dots Protected with Tiopronin: A New Fluorescence System for Cell-Biology Studies. *ChemBioChem* **2005**, *6*, 989–991.

161. Lewin, M.; Carlesso, N.; Tung, C. H.; Tang, X. W.; Corry, D.; Scadden, D. T.; Weissleder, R. TAT Peptide-Derivatized Magnetic Nanoparticles Allow *in Vivo* Tracking and Recovery of Progenitor Cells. *Nat. Biotechnol.* **2000**, *18*, 410–414.

162. Verma, A.; Uzun, O.; Hu, Y. H.; Hu, Y.; Han, H. S.; Watson, N.; Chen, S. L.; Irvine, D. J.; Stellacci, F. Surface-Structure-Regulated Cell-Membrane Penetration by Monolayer-Protected Nanoparticles. *Nat. Mater.* **2008**, *7*, 588–595.

163. Jewell, C. M.; Jung, J. M.; Atukorale, P. U.; Carney, R. P.; Stellacci, F.; Irvine, D. J. Oligonucleotide Delivery by Cell-Penetrating "Striped" Nanoparticles. *Angew. Chem., Int. Ed.* **2011**, *50*, 12312–12315.

164. Brandenberger, C.; Mühlfeld, C.; Ali, Z.; Lenz, A. G.; Schmid, O.; Parak, W. J.; Gehr, P.; Rothen-Rutishauser, B. Quantitative Evaluation of Cellular Uptake and Trafficking of Plain and Polyethylene Glycol-Coated Gold Nanoparticles. *Small* **2010**, *6*, 1669–1678.